other 14-3-3-binding targets, especially aggregation-prone targets.

## Materials and Methods

### Materials

The mammalian expression plasmid carrying FLAG-tagged TRIM32 was generated by PCR using oligonucleotides 5′-CGGGATCCATGGCTGCAGCA-GCAGCTTC-3′ and 5′-CGGAATTCCTATGGGGTGGAATATCTTC-3′ and human TRIM32 cDNA (pOTB7, Funakosi) as template. The PCR fragment was digested with *Bam*HI and *Eco*RI and then inserted into the cloning site of the FLAG-tag vector pCMV-Tag2B (Invitrogen), termed pCMV-TRIM32. The expression plasmids for myc–14-3-3$\eta$ and its V180D mutant or FLAG–14-3-3$\eta$ have been described (Ichimura et al., 2005). The CFP-TRIM32 construct was created by ligating the *Bam*HI/*Eco*RI fragment of pCMV-TRIM32 into the *Bgl*II/*Eco*RI site of pECFP-C1 (Clontech). The deletion and point mutants of TRIM32 were created according to the standard protocol of PCR-based targeted mutagenesis (Ichimura et al., 2002). The 14-3-3$\eta$ protein was prepared by cleavage of GST–14-3-3$\eta$ (Nagaki et al., 2006) with Factor X (Bio-Rad). The catalytic subunit of PKA was isolated from porcine brain (Nagaki et al., 2006). Human TRIM32 was obtained from Abnova. The plasmids shown in supplementary material Fig. S1 were kind gifts from Drs Richard Roth (for AKT1S1–HA), Jennifer Byrne (for EGFP–TPD52L1), Daisuke Koya (for myc–Smurf1), and Danny Reinberg (for FLAG–RNF20) or were made by PCR using TORC2/pSport6 (kindly provided by Dr Yo Takemori, for FLAG–TORC2 in pCMV-Tag2B), pME18SFL3 (Toyobo, for FLAG–WDR20 in pCMV-Tag2B), pCMV-SPORT6 (Funakosi, for FLAG–TFEB in pCMV-Tag2B), or the reported plasmids of CaMKK$\alpha$ [(Ichimura et al., 2008) for myc–CaMKK$\alpha$ in pcDNA3], Nedd4-2 [(Ichimura et al., 2005) for myc–Nedd4-2 in pcDNA3], and TH [(Itagaki et al., 1999) for myc–TH in pcDNA3] as templates. The plasmid for FLAG–AGO1 was kindly provided by Dr Haruhiko Siomi. The PAN-14-3-3 antibody, anti-TRIM32, anti-GST and monoclonal anti-myc were purchased from Santa Cruz Biotechnology. Anti-14-3-3$\eta$ was purchased from Immuno-Biological Laboratories. Polyclonal anti-myc and anti-phospho(Ser/Thr)-PKA substrate were purchased from Cell Signaling. Monoclonal anti-HA and anti-FLAG were purchased from Upstate and Kodak, respectively. Polyclonal anti-FLAG was purchased from Rockland. Monoclonal anti-tubulin was purchased from Sigma.

#### Quantitative proteomics

Quantitative proteomics was carried out as described previously (Ichimura et al., 2008). Six 15-cm dishes of PC12Mh cells (Ichimura et al., 2005) stably expressing MEF-fused 14-3-3 ($\eta$-isoform) were metabolically labeled with [$^{13}$C]Lys/Arg for 12 days. The labeled cells were stimulated with 50 μM forskolin (Sigma) for 20 minutes, lysed in 3 ml of lysis buffer [50 mM Tris-HCl, pH 7.5, 150 mM NaCl, 10% (w/v) glycerol, 100 mM NaF, 10 mM EGTA, 1 mM $Na_3VO_4$, 1% (w/v) Triton X-100, 5 mM $ZnCl_2$, 2 mM phenylmethylsulfonyl fluoride, 10 μg/ml aprotinin, and 1 μg/ml leupeptin] and combined with an equal volume of the lysate from unlabeled, non-stimulated PC12Mh cells. Proteins bound to the expressed MEF-14-3-3$\eta$ were then purified from the combined lysates by the MEF method (Ichimura et al., 2005). The recovered proteins were digested with trypsin and then identified and quantified by two-dimensional liquid chromatography–tandem mass spectrometry using the MASCOT (Matrix Science) and STEM software programs (Shinkawa et al., 2005). For quantification, values were corrected by STEM for an incorporation efficiency of 81% [$^{13}$C]Lys and 70% [$^{13}$C]Arg.

#### Co-immunoprecipitation and pull-down assay

Co-immunoprecipitation analyses were conducted as described previously (Ichimura et al., 2005). HEK293 cells (2–4×10$^6$) were transiently transfected with expression plasmids (each 5 μg) encoding FLAG–TRIM32 or its mutants, with or without myc–14-3-3 and cPKA. After 24 hours, the expressed FLAG–TRIM32 was immunoprecipitated with anti-FLAG–Sepharose (Sigma), washed five times with buffer A [50 mM Tris-HCl, pH 7.5, 150 mM NaCl, 10% (w/v) glycerol and 0.1% (w/v) Triton X-100], and the bound 14-3-3 was released from the beads with 1 mM synthetic phosphopeptide [LSQRQRSTS(*P*)TPNVHA, based on residues 250–265 of human cRaf1). Proteins were then separated by 10% SDS-PAGE and analyzed by western blotting using the specific antibodies indicated in each figure. For GST pull-down experiments, GST–TRIM32 or GST alone (each ~0.5 μg) was incubated with 14-3-3$\eta$ (1 μg) for 20 minutes at 30℃ in 25 μl final volume (50 mM HEPES, pH 7.5, 10 mM magnesium acetate, and 0.1 mM ATP) in the presence or absence of 0.25 μl of the catalytic subunit of PKA. After incubation, glutathione–agarose beads (Pharmacia) were added to the reaction and further incubated for 60 minutes at 4℃. The beads were then washed five times with buffer A, and the precipitated complexes were analyzed by 10% SDS-PAGE followed by western blotting.

#### Immunopurification of 14-3-3 from mouse skeletal muscle and brain

Frozen mouse skeletal muscle and brain were homogenized in 10 volumes of lysis buffer, and the homogenates were centrifuged at 100,000 ***g*** for 30 minutes at 4℃. The cleared lysates (1.5 mg) were incubated with 4 μg of anti-PAN 14-3-3 IgG for 60 minutes at 4℃. Immobilized protein A/G–Sepharose (Santa Cruz Biotechnology) was added, and lysates were further incubated for 60 minutes at 4℃. Immunoprecipitated 14-3-3 complexes were washed five times with buffer A and eluted with SDS-PAGE sample buffer (lacking β-mercaptoethanol).

#### Immunofluorescence microscopy and electron microscopy

HEK293 cells grown on 3.5-cm plates (FluoroDish, World Precision Instruments, Inc.) were transfected with the indicated expression plasmids (each 0.5 μg) for 24 hours using Lipofectamine 2000 (Invitrogen). Transfected cells were rinsed with phosphate-buffered saline (PBS) containing 0.1 g/l $CaCl_2$ and 0.1 g/l $MgCl_2$ [PBS(+)] and fixed with 10% formalin in 70% PBS(+) for 30 minutes at 25℃. The fixed cells were washed four times with PBS, then incubated with 10% fetal bovine serum in PBS for 30 minutes at room temperature and subsequently incubated for 1 hour at room temperature with specific primary antibodies (see figure legends). After washing four times with PBS, the cells were incubated with Alexa-Fluor-488-conjugated (green) and Alexa-Fluor-594-conjugated (red) anti-rabbit or anti-mouse secondary antibodies (Molecular Probes) for 1 hour at room temperature. The stained cells were washed four times with PBS and then visualized using a Delta Vision microscope system (Applied Precision, Inc.).

For electron microscopy, HEK293 cells transfected with FLAG–TRIM32 were fixed for 1 hour at room temperature with 2.5% glutaraldehyde (TAAB Laboratories Equipment Ltd) in 0.1 M sodium phosphate buffer (pH 7.2), washed with PBS, and postfixed with 1% osmium tetroxide for 1 hour at room temperature in 0.1 M sodium phosphate buffer. Cells were then dehydrated with ethanol up to 100%, and finally embedded with Quetol 812-based resin (Nisshin EM). Ultrathin sections were stained with uranyl acetate and lead citrate and mounted on 150-mesh copper grids. Electron microscopy images were collected with a TEM H7100 (Hitachi Ltd) and scanned with a SUPER COOLSCAN 8000 (Nikon). Counting FLAG–TRIM32-expressing and myc–14-3-3-expressing cells revealed that the efficiency of FLAG–TRIM32 expression was 20–40% and that more than 90% of the FLAG–TRIM32-positive cells were also positive for myc-14-3-3 expression.

#### In-cell ubiquitylation assay

The ubiquitylation assay was performed as described previously (Ichimura et al., 2005). HEK293 cells (2–4×10$^6$) were co-transfected with the indicated expression plasmids (each 5 μg) for 48 hours and lysed in 1% SDS. Samples were subsequently diluted with 9 volumes of lysis buffer and incubated with anti-FLAG–Sepharose beads (Sigma) or with anti-HA affinity matrix (Roche). The beads were washed five times with buffer A, and bound proteins were analyzed by 7.5% or 10% SDS-PAGE followed by western blotting with monoclonal anti-HA or anti-FLAG.

#### Sucrose density gradient

HEK293 cells (2–4×10$^6$) were transfected with the indicated expression plasmids (each 5 μg) for 36 hours and homogenized in PBS. The homogenates (50 μg protein) were loaded on to a sucrose density gradient (5–20%, w/v) and centrifuged at 100,000 ***g*** for 18 hours at 4℃. The samples were fractionated from the bottom of the tubes, precipitated with 10% trichloroacetic acid, and subjected to 10% SDS-PAGE followed by western blotting with anti-TRIM32. The gel image was quantified with an E-Graph densitometer (ATTO) and the results were expressed as a percentage of total amounts of protein in each experiment.

#### Retroviral infection and cell counting

Retrovirus expression vectors for FLAG–TRIM32 wild-type (WT) and S651A point mutant (S651A) were constructed with pMX-puro (Kano et al., 2008). NIH3T3 fibroblasts were infected with retroviruses produced by Plat-E packaging cells as described previously (Kano et al., 2008). Infected cells were seeded at 1×10$^4$ cells per well in six-well plates and harvested for determination of cell number at various times.

## Acknowledgements

We thank H. Siomi, R. Roth, J. Byrne, D. Koya, D. Reinberg and Y. Takemori for plasmids, and L. Greene for PC12 cells. We also thank S. Yamada, K. Kakiuchi, J. Yoshida, C. Uchida, K. Nishijima and Y. Komata for help in doing some experiments.

## Author contributions

T.I. carried out most of the experiments. M.T., I.S., H.K. and T.I. helped with mass spectrometry and immunocytochemical analyses. T.S. and S.H. contributed in the generation of stable NIH3T3 cells. T.I. and N.H. evaluated experiments and wrote the manuscript. All authors were involved in data discussions and preparing the final version of the manuscript.

## Funding

This work was supported by the Ministry of Education, Culture, Sports, Science and Technology of Japan through Grants-in-Aid for Scientific Research [grant numbers 21570213 to T.I.; 24112006 and 24390065 to S.H.]; the Integrated Proteomics System Project, Pioneer Research on Genome the Frontier; the Mitsubishi Pharma Research foundation; the Suhara Memorial Foundation; and the Sumitomo Foundation.

Supplementary material available online at
http://jcs.biologists.org/lookup/suppl/doi:10.1242/jcs.122069/-/DC1

## References

**Albor, A., El-Hizawi, S., Horn, E. J., Laederich, M., Frosk, P., Wrogemann, K. and Kulesz-Martin, M.** (2006). The interaction of Piasy with Trim32, an E3-ubiquitin ligase mutated in limb-girdle muscular dystrophy type 2H, promotes Piasy degradation and regulates UVB-induced keratinocyte apoptosis through NFkappaB. *J. Biol. Chem.* **281**, 25850-25866.

**Bhalla, V., Daidié, D., Li, H., Pao, A. C., LaGrange, L. P., Wang, J., Vandewalle, A., Stockand, J. D., Staub, O. and Pearce, D.** (2005). Serum- and glucocorticoid-regulated kinase 1 regulates ubiquitin ligase neural precursor cell-expressed, developmentally down-regulated protein 4-2 by inducing interaction with 14-3-3. *Mol. Endocrinol.* **19**, 3073-3084.

**Campbell, E. M., Dodding, M. P., Yap, M. W., Wu, X., Gallois-Montbrun, S., Malim, M. H., Stoye, J. P. and Hope, T. J.** (2007). TRIM5 alpha cytoplasmic bodies are highly dynamic structures. *Mol. Biol. Cell* **18**, 2102-2111.

**Chen, H. K., Fernandez-Funez, P., Acevedo, S. F., Lam, Y. C., Kaytor, M. D., Fernandez, M. H., Aitken, A., Skoulakis, E. M., Orr, H. T., Botas, J. et al.** (2003). Interaction of Akt-phosphorylated ataxin-1 with 14-3-3 mediates neurodegeneration in spinocerebellar ataxia type 1. *Cell* **113**, 457-468.

**Coblitz, B., Wu, M., Shikano, S. and Li, M.** (2006). C-terminal binding: an expanded repertoire and function of 14-3-3 proteins. *FEBS Lett.* **580**, 1531-1535.

**Diaz-Griffero, F., Li, X., Javanbakht, H., Song, B., Welikala, S., Stremlau, M. and Sodroski, J.** (2006). Rapid turnover and polyubiquitylation of the retroviral restriction factor TRIM5. *Virology* **349**, 300-315.

**Dougherty, M. K. and Morrison, D. K.** (2004). Unlocking the code of 14-3-3. *J. Cell Sci.* **117**, 1875-1884.

**Edwards, T. A., Wilkinson, B. D., Wharton, R. P. and Aggarwal, A. K.** (2003). Model of the brain tumor-Pumilio translation repressor complex. *Genes Dev.* **17**, 2508-2513.

**Fridell, R. A., Harding, L. S., Bogerd, H. P. and Cullen, B. R.** (1995). Identification of a novel human zinc finger protein that specifically interacts with the activation domain of lentiviral Tat proteins. *Virology* **209**, 347-357.

**Frosk, P., Weiler, T., Nylen, E., Sudha, T., Greenberg, C. R., Morgan, K., Fujiwara, T. M. and Wrogemann, K.** (2002). Limb-girdle muscular dystrophy type 2H associated with mutation in TRIM32, a putative E3-ubiquitin-ligase gene. *Am. J. Hum. Genet.* **70**, 663-672.

**Ganguly, S., Weller, J. L., Ho, A., Chemineau, P., Malpaux, B. and Klein, D. C.** (2005). Melatonin synthesis: 14-3-3-dependent activation and inhibition of arylalkylamine N-acetyltransferase mediated by phosphoserine-205. *Proc. Natl. Acad. Sci. USA* **102**, 1222-1227.

**Ganser-Pornillos, B. K., Chandrasekaran, V., Pornillos, O., Sodroski, J. G., Sundquist, W. I. and Yeager, M.** (2011). Hexagonal assembly of a restricting TRIM5alpha protein. *Proc. Natl. Acad. Sci. USA* **108**, 534-539.

**Gelperin, D., Weigle, J., Nelson, K., Roseboom, P., Irie, K., Matsumoto, K. and Lemmon, S.** (1995). 14-3-3 proteins: potential roles in vesicular transport and Ras signaling in Saccharomyces cerevisiae. *Proc. Natl. Acad. Sci. USA* **92**, 11539-11543.

**Hatakeyama, S.** (2011). TRIM proteins and cancer. *Nat. Rev. Cancer* **11**, 792-804.

**Horn, E. J., Albor, A., Liu, Y., El-Hizawi, S., Vanderbeek, G. E., Babcock, M., Bowden, G. T., Hennings, H., Lozano, G., Weinberg, W. C. et al.** (2004). RING protein Trim32 associated with skin carcinogenesis has anti-apoptotic and E3-ubiquitin ligase properties. *Carcinogenesis* **25**, 157-167.

**Hwang, C. Y., Holl, J., Rajan, D., Lee, Y., Kim, S., Um, M., Kwon, K. S. and Song, B.** (2010). Hsp70 interacts with the retroviral restriction factor TRIM5alpha and assists the folding of TRIM5alpha. *J. Biol. Chem.* **285**, 7827-7837.

**Ichimura, T., Wakamiya-Tsuruta, A., Itagaki, C., Taoka, M., Hayano, T., Natsume, T. and Isobe, T.** (2002). Phosphorylation-dependent interaction of kinesin light chain 2 and the 14-3-3 protein. *Biochemistry* **41**, 5566-5572.

**Ichimura, T., Yamamura, H., Sasamoto, K., Tominaga, Y., Taoka, M., Kakiuchi, K., Shinkawa, T., Takahashi, N., Shimada, S. and Isobe, T.** (2005). 14-3-3 proteins modulate the expression of epithelial Na+ channels by phosphorylation-dependent interaction with Nedd4-2 ubiquitin ligase. *J. Biol. Chem.* **280**, 13187-13194.

**Ichimura, T., Taoka, M., Hozumi, Y., Goto, K. and Tokumitsu, H.** (2008). 14-3-3 Proteins directly regulate Ca(2+)/calmodulin-dependent protein kinase kinase alpha through phosphorylation-dependent multisite binding. *FEBS Lett.* **582**, 661-665.

**Itagaki, C., Isobe, T., Taoka, M., Natsume, T., Nomura, N., Horigome, T., Omata, S., Ichinose, H., Nagatsu, T., Greene, L. A. et al.** (1999). Stimulus-coupled interaction of tyrosine hydroxylase with 14-3-3 proteins. *Biochemistry* **38**, 15673-15680.

**Johnston, M., Geoffroy, M. C., Sobala, A., Hay, R. and Hutvagner, G.** (2010). HSP90 protein stabilizes unloaded argonaute complexes and microscopic P-bodies in human cells. *Mol. Biol. Cell* **21**, 1462-1469.

**Kano, S., Miyajima, N., Fukuda, S. and Hatakeyama, S.** (2008). Tripartite motif protein 32 facilitates cell growth and migration via degradation of Abl-interactor 2. *Cancer Res.* **68**, 5572-5580.

**Kentsis, A., Gordon, R. E. and Borden, K. L.** (2002). Control of biochemical reactions through supramolecular RING domain self-assembly. *Proc. Natl. Acad. Sci. USA* **99**, 15404-15409.

**Kudryashova, E., Kudryashov, D., Kramerova, I. and Spencer, M. J.** (2005). Trim32 is a ubiquitin ligase mutated in limb girdle muscular dystrophy type 2H that binds to skeletal muscle myosin and ubiquitinates actin. *J. Mol. Biol.* **354**, 413-424.

**Kudryashova, E., Wu, J., Havton, L. A. and Spencer, M. J.** (2009). Deficiency of the E3 ubiquitin ligase TRIM32 in mice leads to a myopathy with a neurogenic component. *Hum. Mol. Genet.* **18**, 1353-1367.

**Kudryashova, E., Struyk, A., Mokhonova, E., Cannon, S. C. and Spencer, M. J.** (2011). The common missense mutation D489N in TRIM32 causing limb girdle muscular dystrophy 2H leads to loss of the mutated protein in knock-in mice resulting in a Trim32-null phenotype. *Hum. Mol. Genet.* **20**, 3925-3932.

**Li, X., Yeung, D. F., Fiegen, A. M. and Sodroski, J.** (2011). Determinants of the higher order association of the restriction factor TRIM5alpha and other tripartite motif (TRIM) proteins. *J. Biol. Chem.* **286**, 27959-27970.

**Locke, M., Tinsley, C. L., Benson, M. A. and Blake, D. J.** (2009). TRIM32 is an E3 ubiquitin ligase for dysbindin. *Hum. Mol. Genet.* **18**, 2344-2358.

**Nagaki, K., Yamamura, H., Shimada, S., Saito, T., Hisanaga, S., Taoka, M., Isobe, T. and Ichimura, T.** (2006). 14-3-3 Mediates phosphorylation-dependent inhibition of the interaction between the ubiquitin E3 ligase Nedd4-2 and epithelial Na+ channels. *Biochemistry* **45**, 6733-6740.

**Nisole, S., Stoye, J. P. and Saïb, A.** (2005). TRIM family proteins: retroviral restriction and antiviral defence. *Nat. Rev. Microbiol.* **3**, 799-808.

**Okada, N., Yabuta, N., Suzuki, H., Aylon, Y., Oren, M. and Nojima, H.** (2011). A novel Chk1/2-Lats2-14-3-3 signaling pathway regulates P-body formation in response to UV damage. *J. Cell Sci.* **124**, 57-67.

**Pertel, T., Hausmann, S., Morger, D., Züger, S., Guerra, J., Lascano, J., Reinhard, C., Santoni, F. A., Uchil, P. D., Chatel, L. et al.** (2011). TRIM5 is an innate immune sensor for the retrovirus capsid lattice. *Nature* **472**, 361-365.

**Reymond, A., Meroni, G., Fantozzi, A., Merla, G., Cairo, S., Luzi, L., Riganelli, D., Zanaria, E., Messali, S., Cainarca, S. et al.** (2001). The tripartite motif family identifies cell compartments. *EMBO J.* **20**, 2140-2151.

**Roberts, R. L., Mösch, H. U. and Fink, G. R.** (1997). 14-3-3 proteins are essential for RAS/MAPK cascade signaling during pseudohyphal development in S. cerevisiae. *Cell* **89**, 1055-1065.

**Ryu, Y. S., Lee, Y., Lee, K. W., Hwang, C. Y., Maeng, J. S., Kim, J. H., Seo, Y. S., You, K. H., Song, B. and Kwon, K. S.** (2011). TRIM32 protein sensitizes cells to tumor necrosis factor (TNFα)-induced apoptosis via its RING domain-dependent E3 ligase activity against X-linked inhibitor of apoptosis (XIAP). *J. Biol. Chem.* **286**, 25729-25738.

**Schwamborn, J. C., Berezikov, E. and Knoblich, J. A.** (2009). The TRIM-NHL protein TRIM32 activates microRNAs and prevents self-renewal in mouse neural progenitors. *Cell* **136**, 913-925.

**Shinkawa, T., Taoka, M., Yamauchi, Y., Ichimura, T., Kaji, H., Takahashi, N. and Isobe, T.** (2005). STEM: a software tool for large-scale proteomic data analyses. *J. Proteome Res.* **4**, 1826-1831.

**Song, B., Diaz-Griffero, F., Park, D. H., Rogers, T., Stremlau, M. and Sodroski, J.** (2005). TRIM5alpha association with cytoplasmic bodies is not required for antiretroviral activity. *Virology* **343**, 201-211.

**Stoecklin, G., Stubbs, T., Kedersha, N., Wax, S., Rigby, W. F., Blackwell, T. K. and Anderson, P.** (2004). MK2-induced tristetraprolin:14-3-3 complexes prevent stress granule association and ARE-mRNA decay. *EMBO J.* **23**, 1313-1324.

**Urano, T., Saito, T., Tsukui, T., Fujita, M., Hosoi, T., Muramatsu, M., Ouchi, Y. and Inoue, S.** (2002). Efp targets 14-3-3 sigma for proteolysis and promotes breast tumour growth. *Nature* **417**, 871-875.

**Vincenz, C. and Dixit, V. M.** (1996). 14-3-3 proteins associate with A20 in an isoform-specific manner and function both as chaperone and adapter molecules. *J. Biol. Chem.* **271**, 20029-20034.

**Yokota, T., Mishra, M., Akatsu, H., Tani, Y., Miyauchi, T., Yamamoto, T., Kosaka, K., Nagai, Y., Sawada, T. and Heese, K.** (2006). Brain site-specific gene expression analysis in Alzheimer's disease patients. *Eur. J. Clin. Invest.* **36**, 820-830.

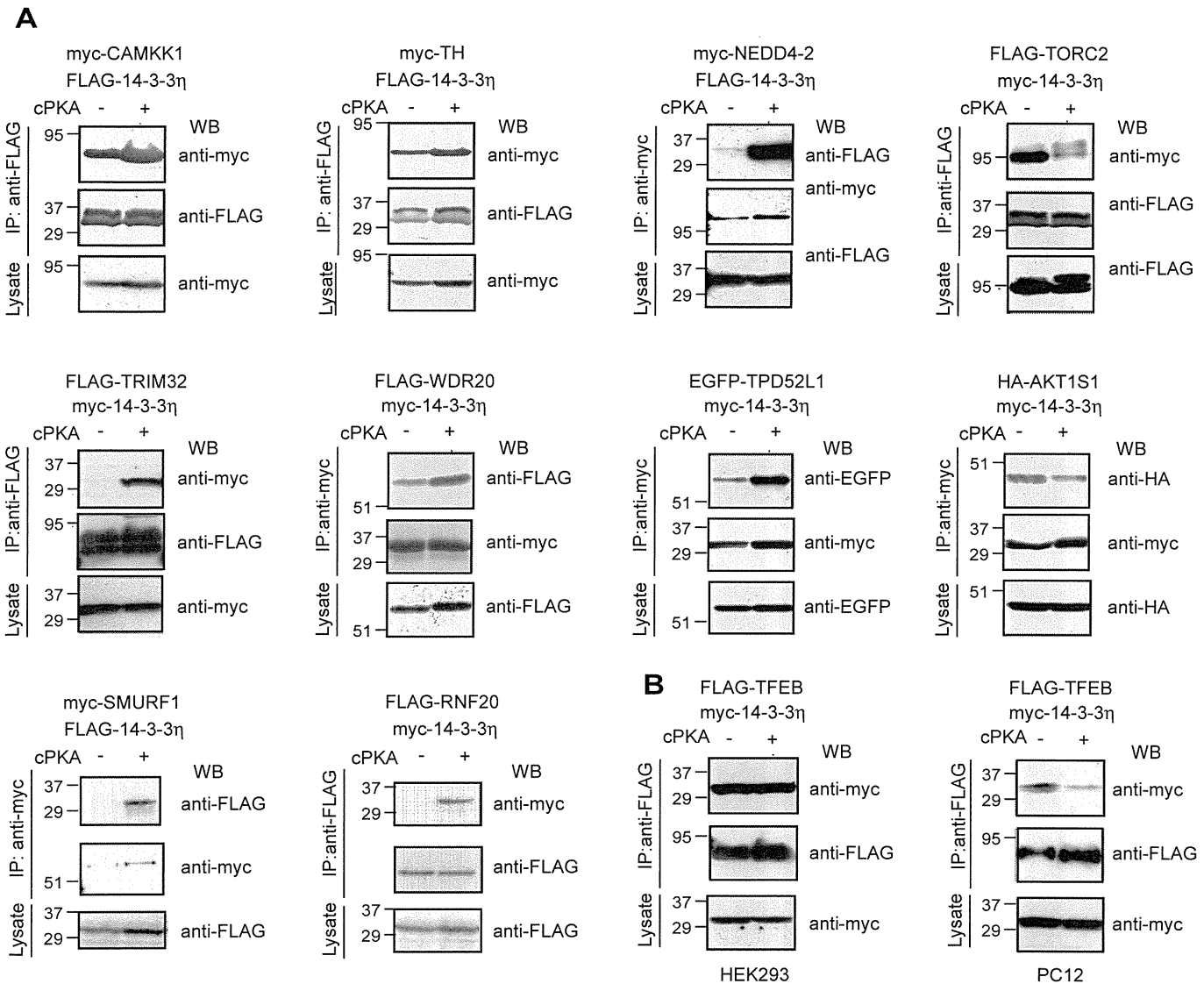


**Fig. S1. Regulation of 14-3-3 interactions by cPKA.** (A) HEK293 cells were transfected with the indicated plasmids with (+) or without (–) cPKA (5 μg each). After 24 h, the expressed proteins were immunoprecipitated (IP) with anti-FLAG or anti-myc, and the immunocomplexes were analyzed by 10% SDS-PAGE followed by western blotting (WB) with the indicated antibodies (top and middle panels, respectively). The cell lysates (20 μg of protein each) were also analyzed by WB to determine protein levels of co-precipitated proteins (bottom panels). Molecular size markers, in kDa, are indicated to the left. (B) HEK293 cells (left panels) or PC12 cells (right panels) were co-transfected with the indicated constructs and analyzed by WB as in panel A.

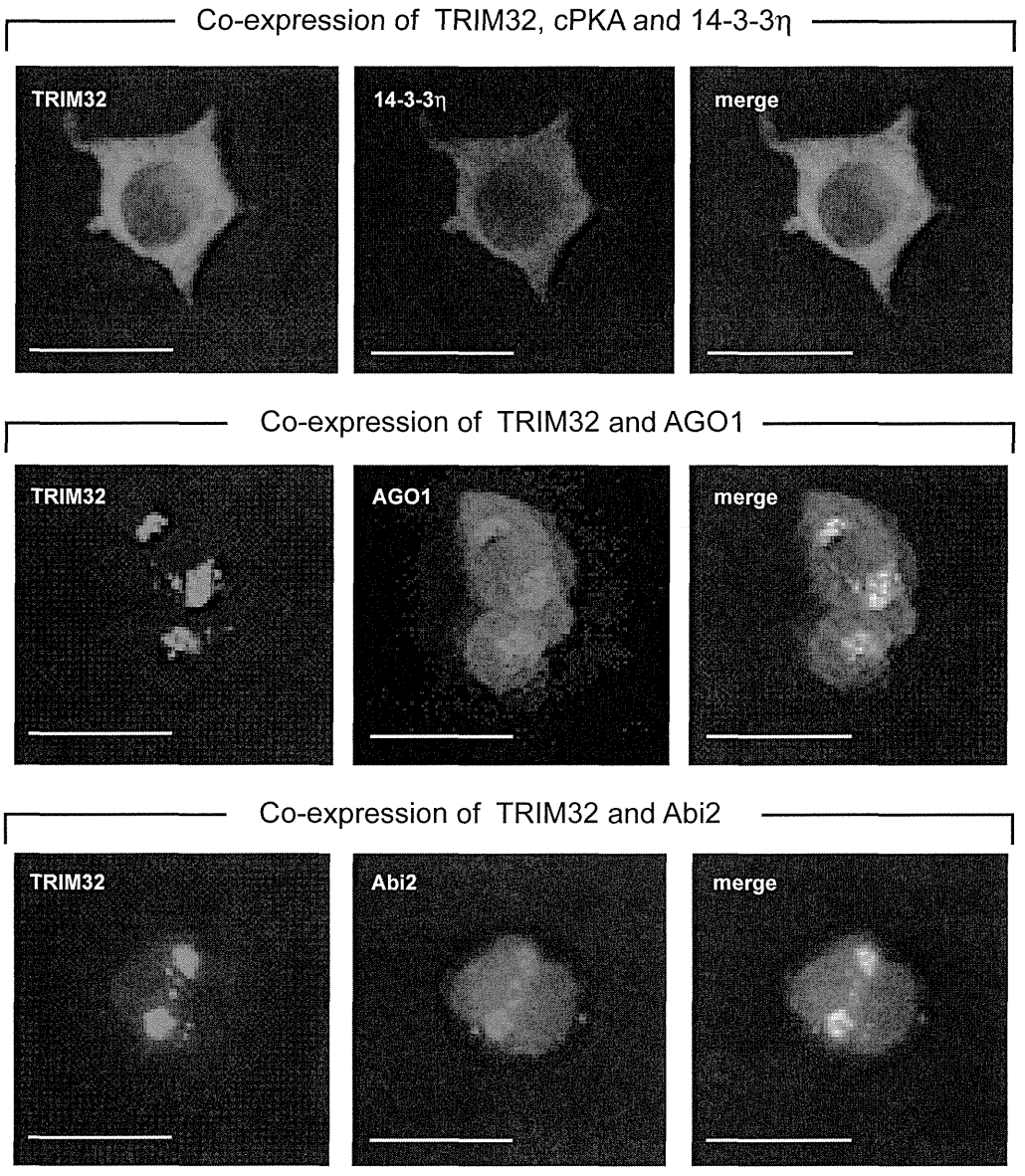


**Fig. S2. Coexpression of 14-3-3η, but not AGO1 and Abi2, suppresses the formation of TRIM32 CBs.** HEK293 cells were co-transfected with the indicated constructs (myc-TRIM32, FLAG-14-3-3η, FLAG-AGO1, FLAG-Abi2, cPKA), and after 24 h the cells were stained with monoclonal mouse anti-myc (green) and polyclonal rabbit anti-FLAG (red). Note that coexpression of 14-3-3η, but not AGO1 and ABi2, specifically disperses the TRIM32 protein throughout the cytoplasm. Scale bars: 10 μm.

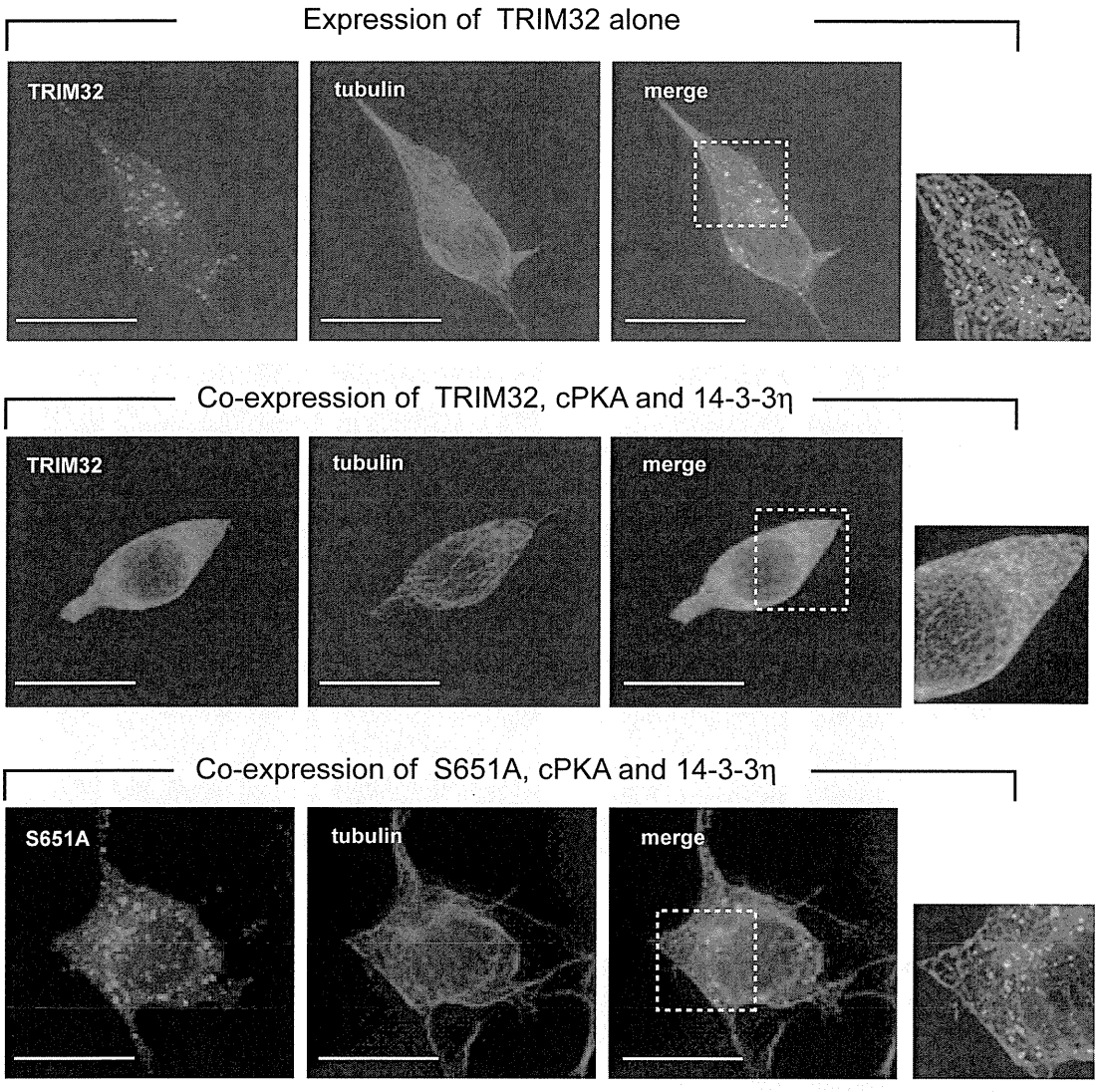


**Fig. S3. Coexpression of 14-3-3η suppresses the association of TRIM32 with microtubules.** HEK293 cells were co-transfected with the indicated constructs (FLAG-TRIM32, FLAG-S651A, myc-14-3-3η, cPKA), and after 12–16 h the cells were stained with polyclonal anti-FLAG-TRIM32 (green) and monoclonal anti-α-tubulin (red). Scale bars: 10 μm.

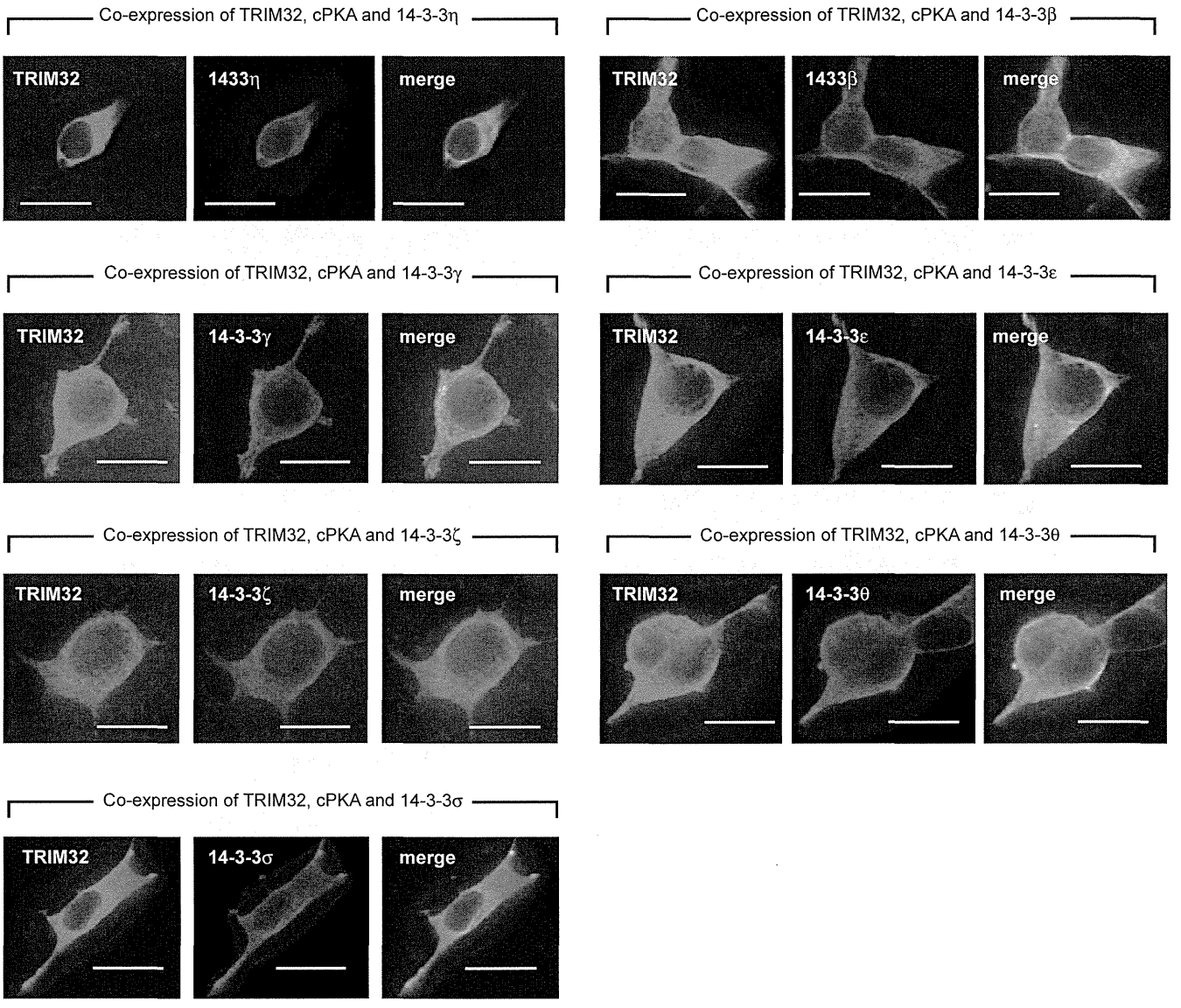


**Fig. S4. All mammalian 14-3-3 isoforms affect the subcellular distribution of TRIM32.** HEK293 cells were co-transfected with the indicated constructs (FLAG-TRIM32, myc-14-3-3s, cPKA), and after 24 h the cells were stained as in Fig. 3B. Scale bars: 10 μm.

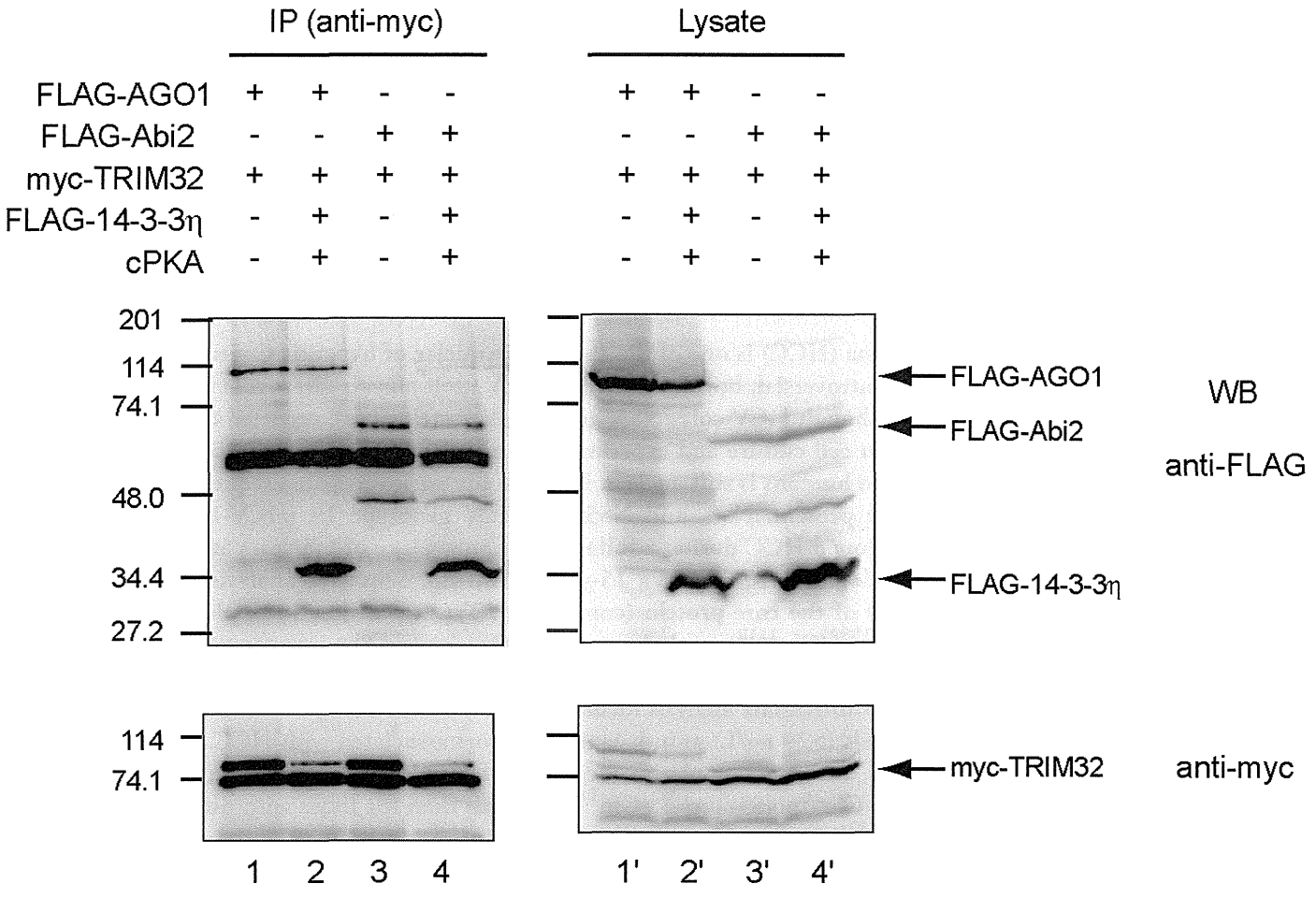


**Fig. S5. 14-3-3 binding does not significantly disrupt the interaction of TRIM32 with AGO1 or Abi2.** HEK293 cells transiently transfected with the indicated plasmids (5 μg each) were lysed with 1% Triton X-100 and then subjected to immunoprecipitation (IP) with anti-myc after normalizing levels of expressed proteins in each IP experiment. The amounts of myc- and FLAG-tagged proteins in the immunoprecipitates (left panels) and in lysates (right panels) were analyzed by western blotting (WB) with the indicated antibodies. Molecular size markers, in kDa, are indicated to the left.

**Table S1. List of 14-3-3-associated proteins consistently identified in at least two LC-MS/MS analyses**

Download Table S1

HEPATOLOGY
Official Journal of the American Association for the Study of Liver Diseases

# Polymorphisms of the Core, NS3, and NS5a Proteins of Hepatitis C Virus Genotype 1b Associate With Development of Hepatocellular Carcinoma

Ahmed El-Shamy,[1,2]* Michiko Shindo,[3]** Ikuo Shoji,[1] Lin Deng,[1] Tadao Okuno,[3] and Hak Hotta[1]

**Hepatocellular carcinoma (HCC) is one of the common sequelae of hepatitis C virus (HCV) infection. It remains controversial, however, whether HCV itself plays a direct role in the development of HCC. Although HCV core, NS3, and NS5A proteins were reported to display tumorigenic activities in cell culture and experimental animal systems, their clinical impact on HCC development in humans is still unclear. In this study we investigated sequence polymorphisms in the core protein, NS3, and NS5A of HCV genotype 1b (HCV-1b) in 49 patients who later developed HCC during a follow-up of an average of 6.5 years and in 100 patients who did not develop HCC after a 15-year follow-up. Sequence analysis revealed that Gln at position 70 of the core protein (core-Gln$^{70}$), Tyr at position 1082 plus Gln at 1112 of NS3 (NS3-Tyr$^{1082}$/Gln$^{1112}$), and six or more mutations in the interferon/ribavirin resistance-determining region of NS5A (NS5A-IRRDR≥6) were significantly associated with development of HCC. Multivariate analysis identified core-Gln$^{70}$, NS3-Tyr$^{1082}$/Gln$^{1112}$, and α-fetoprotein (AFP) levels (>20 ng/L) as independent factors associated with HCC. Kaplan-Meier analysis revealed a higher cumulative incidence of HCC for patients infected with HCV isolates with core-Gln$^{70}$, NS3-Tyr$^{1082}$/Gln$^{1112}$ or both than for those with non-(Gln$^{70}$ plus NS3-Tyr$^{1082}$/Gln$^{1112}$). In most cases, neither the residues at position 70 of the core protein nor positions 1082 and 1112 of the NS3 protein changed during the observation period. *Conclusion*: HCV isolates with core-Gln$^{70}$ and/or NS3-Tyr$^{1082}$/Gln$^{1112}$ are more closely associated with HCC development compared to those with non-(Gln$^{70}$ plus NS3-Tyr$^{1082}$/Gln$^{1112}$). (HEPATOLOGY 2013;58:555-563)**

See Editorial on Page 491

Hepatitis C virus (HCV) is a major etiologic agent of chronic hepatitis worldwide, with the estimated number of infected individuals being more than 180 million. Approximately 15% to 20% of chronically infected individuals undergo liver cirrhosis in a decade or so after infection, with hepatocellular carcinoma (HCC) arising from cirrhosis at an estimated rate of 1% to 4% per year.[1-3] Several host factors such as male gender, older age, elevated α-fetoprotein (AFP) level, advanced liver fibrosis as well as nonresponsiveness to interferon (IFN) therapy have been reported as important predictors of HCC development.[4,5] Recently, a host genetic factor, i.e., the *DEPDC5* locus polymorphism, was reported to be associated with progression to HCC in HCV-infected individuals.[6] On the other hand, it remains controversial as to whether HCV itself plays a direct role in the development of HCC. Experimental data suggest that HCV contributes to HCC by modulating pathways that promote malignant transformation of hepatocytes. HCV core, NS3, and NS5A proteins were shown to be involved in a

*Abbreviations: HCC, hepatocellular carcinoma; HCV, hepatitis C virus; IFN, interferon; IRRDR, interferon/ribavirin resistance-determining region; ISDR, interferon sensitivity-determining region.*

*From the [1]Division of Microbiology, Kobe University Graduate School of Medicine, Kobe, Japan; [2]Department of Virology, Suez Canal University Faculty of Veterinary Medicine, Ismalia, Egypt; and [3]Department of Gastroenterology, Akashi City Hospital, Akashi, Japan.*

*Received September 3, 2012; accepted December 9, 2012.*

*Supported in part by Health and Labour Sciences Research Grants from the Ministry of Health, Labour and Welfare, Japan, and a SATREPS Grant from Japan Science and Technology Agency (JST) and Japan International Cooperation Agency (JICA). This study was also carried out as part of Japan Initiative for Global Research Network on Infectious Diseases (J-GRID), Ministry of Education, Culture, Sports, Science and Technology, Japan, and the Global Center of Excellence (G-COE) Program at Kobe University Graduate School of Medicine.*

**These authors contributed equally to this work.*

*Current address for Ahmed El-Shamy: Division of Liver Diseases, Mount Sinai School of Medicine, New York, New York, USA.*

*Current address for Michiko Shindo and Tadao Okuno: Okuno Gastroenterology Clinic, Akashi, Hyogo, Japan.*

number of potentially oncogenic pathways in cell culture and experimental animal systems.[7] HCV core protein rendered cultured cells more resistant to apoptosis[8,9] and promoted *ras* oncogene-mediated transformation.[10,11] Moreover, transgenic mice expressing the HCV core protein in the liver developed HCC.[12] However, the clinical impact of HCV proteins on HCC development in humans and whether all HCV isolates are equally associated with HCC is yet to be determined. In a clinical setting, HCV core protein mutations at positions 70 ($Gln^{70}$) and/or 91 ($Met^{91}$) were closely associated with HCC development.[13-16] $Gln^{70}$ and/or $Met^{91}$ were also linked to resistance to PEG-IFN/ribavirin (RBV) treatment.[17-20] In addition, we and other investigators reported that an N-terminal part of the NS3 protein has the capacity to transform NIH3T3 and rat fibroblast cells[21,22] and to render NIH3T3 cells more resistant to DNA damage-induced apoptosis, which is thought to be a prerequisite for malignant transformation of the cell.[23] Also, the NS5A protein is a pleiotropic protein with key roles in both viral RNA replication and modulation of the host cell functions.[24] In particular, the links between NS5A and the IFN responses have been widely discussed. It was proposed initially that sequence variations within a region in NS5A spanning from amino acids (aa) 2209 to 2248, called the IFN sensitivity-determining region (ISDR), were correlated with IFN responsiveness.[25] Subsequently, in the era of PEG-IFN/RBV combination therapy, we identified a new region near the C-terminus of NS5A spanning from aa 2334 to 2379, which we referred to as the IFN/RBV resistance-determining region (IRRDR).[26,27] The degree of sequence variations within the IRRDR was significantly associated with the clinical outcome of PEG-IFN/RBV therapy. In the context of HCC, several retrospective studies suggested that IFN-based therapy might reduce the risk of HCC development.[4,28-30]

In an attempt to clarify whether viral factors, in particular those within the core, NS3, and NS5A proteins, are involved in HCC development, we carried out a comparative analysis of the aa sequences obtained from HCV patients who developed HCC and those who did not. In addition, we studied the sequence evolution of these genes in the interval between chronic hepatitis C and HCC development over a period of 15 years.

## Patients and Methods

***Ethics Statement.*** The study protocol, which conforms to the provisions of the 1975 Declaration of Helsinki, was approved beforehand by the Ethic Committees in Akashi City Hospital and Kobe University Graduate School of Medicine, and written informed consent was obtained from each patient enrolled in this study.

***Patients.*** A total of 49 HCV-infected patients who developed HCC (HCC group) were retrospectively examined. They were followed up (from 1988 to 2003) with an average period until HCC development being 6.5 ± 2.9 years. Paired serum samples at the time of chronic hepatitis C (pre-HCC sample) and HCC development (post-HCC sample) were collected. As a control group, 100 HCV-infected patients who were followed up over a period of 15 years (from 1988 to 2003) without HCC development were retrospectively examined. Serum samples of the control group were available at the time of first visit to the clinic. All patients enrolled in this study were chronically infected with HCV genotype 1b (HCV-1b). HCV subtype was determined as reported previously.[31] Serum HCV RNA titers were quantitated by reverse-transcription polymerase chain reaction (RT-PCR0 with an internal RNA standard derived from the 5′ noncoding region of HCV (Amplicor HCV Monitor test, v. 2.0, Roche Diagnostics, Tokyo, Japan). All patients underwent liver biopsy and were diagnosed as chronic hepatitis. All HCC and 68% (68/100) of non-HCC patients received IFN-monotherapy, either natural IFN alpha (Sumiferon, Dainipponsumitomo Pharmaceutical, Osaka, Japan) at a dose of 6 million units (MU) or recombinant IFN alpha 2b (Intron A; Schering-Plough, Osaka, Japan) at a dose of 10 MU, 3 times a week for 6 months. All HCC patients were nonresponders (NR), who had detectable viremia during the entire course of IFN treatment. On the other hand, 18 (26%) of the 68 non-HCC patients treated with IFN achieved HCV RNA negativity at the end of treatment followed by rebound viremia within 6 months after the treatment and, therefore, they were referred to as relapsers. The other 50 IFN-treated, non-HCC patients were NR. The remaining 32 non-HCC patients did not receive IFN. All patients were

*Address reprint requests to: Hak Hotta, M.D., Ph.D., Division of Microbiology, Kobe University Graduate School of Medicine, 7-5-1 Kusunoki-cho, Chuo-ku, Kobe 650-0017, Japan. E-mail: hotta@kobe-u.ac.jp; fax: +81-78-382-5519.*



*View this article online at wileyonlinelibrary.com.*
*DOI 10.1002/hep.26205*
*Potential conflict of interest: Nothing to report.*

seen every 2 months and tested for liver function markers during the follow-up period.

***Sequence Analysis of HCV Core, NS3, and NS5A Proteins.*** HCV RNA was extracted from 140 $\mu$L of serum using a commercially available kit (QIAmp viral RNA kit; Qiagen, Tokyo, Japan). The core, NS3, and NS5A regions of the HCV genome were amplified as described elsewhere.[26,32-34] The sequences of the amplified fragments were determined by direct sequencing. The aa sequences were deduced and aligned using GENETYX Win software version 7.0 (GENETYX, Tokyo, Japan). The numbering of aa was according to the polyprotein of the prototype of HCV-1b; HCV-J.[35]

***Statistical Analysis.*** Statistical differences in the baseline parameters of HCC and control groups were determined by Student's $t$ test for numerical variables and Fisher's exact probability or chi-square tests for categorical variables. Likewise, statistical differences in viral mutations between HCC and control groups were determined by Fisher's exact probability test. Kaplan-Meier analysis was performed to estimate the cumulative incidence of HCC. The data obtained were evaluated by the log-rank test. Univariate and multivariate logistic analyses were performed to identify variables that independently associated with HCC development. Variables with $P < 0.1$ in univariate analysis were included in a backward stepwise multivariate logistic regression analysis. The odds ratios and 95% confidence intervals (95% CI) were calculated. All statistical analyses were performed using SPSS v. 16 software (Chicago, IL). Unless otherwise stated, $P < 0.05$ was considered statistically significant.

***Nucleotide Sequence Accession Numbers.*** The sequence data reported in this article have been deposited in the DDBJ/EMBL/GenBank nucleotide sequence databases with the accession numbers AB719460 through AB719842.

## Results

***Demographic Characteristics of HCC and Control Groups.*** The clinical characteristics of HCC and control groups are shown in Table 1. The HCC group had significantly higher titers of ALT, AST, and AFP, and higher fibrosis staging score than that of the control group. There was no significant difference in viremia titers between the two groups.

***Correlation Between Core Protein Sequence Polymorphism and HCC Development.*** HCV core protein sequences were obtained from all (49/49) and 94% (94/100) of pre-HCC and control patients' sera, respectively. Comparative sequence analysis revealed that 22 (45%) of 49 HCV isolates in the pre-HCC sera (pre-HCC isolates) and 59 (63%) of 94 HCV isolates from the control group (control isolates) had wild-core ($Arg^{70}/Leu^{91}$) (Table 2). The difference between HCC and control groups was hovering at a statistically significant level ($P = 0.05$). When the sequence pattern at position 70 alone was examined, a stronger association with HCC was observed. We found that 21 (43%) of 49 pre-HCC isolates had $Gln^{70}$ while only 13 (14%) of 94 control isolates did ($P = 0.0002$). On the other hand, there was no significant correlation between sequence pattern at position 91 and HCC. Thus, a single mutation at position 70 ($Gln^{70}$) was the only polymorphic factor within core protein that was significantly associated with HCC development. It should be noted that there was no significant correlation between $Gln^{70}$ and the degree of fibrosis progression (data not shown).

**Table 1. Demographic Characteristics of HCC and Control Groups**

| Factor | HCC | Control | P Value |
|---|---|---|---|
| Age | 57.3 ± 7.0* | 56.4 ± 8.3 | 0.54 |
| Sex (male/female) | 31/18 | 54/46 | 0.29 |
| ALT (IU/L) | 159.4 ± 79.8 | 129.7 ± 51.5 | 0.007 |
| AST (IU/L) | 113.0 ± 62.2 | 91.6 ± 44.1 | 0.017 |
| AFP (ng/L) | 29.1 ± 33.7 | 18.4 ± 4.4 | 0.002 |
| Platelets (x $10^4/mm^3$) | 16.2 ± 2.8 | 16.2 ± 2.4 | 0.88 |
| Inflammation grading score | 8.7 ± 0.9 | 8.4 ± 1.2 | 0.05 |
| Fibrosis staging score | 2.4 ± 0.5 | 2.2 ± 0.5 | 0.02 |
| HCV-RNA (KIU/mL) | 593.4 ± 112.3 | 618.1 ± 95.9 | 0.17 |

*Mean ± SD. HCC, hepatocellular carcinoma; ALT, alanine aminotransferase; AST, aspartate transaminase; AFP; α-fetoprotein.

***Correlation Between NS3 Protein Sequence Polymorphism and HCC Development.*** Sequences of NS3 serine protease domain (aa 1027 to 1146) were obtained from 94% (46/49) and 93% (93/100) of pre-HCC and control isolates, respectively. We found that 29 (63%) of 46 pre-HCC isolates had Tyr and Gln at positions 1082 and 1112, respectively ($Tyr^{1082}/Gln^{1112}$), while 39 (42%) of 93 control isolates did (Table 2). The difference in the proportion between pre-HCC and control isolates was statistically significant ($P = 0.029$). On the other hand, there was no significant correlation between $Tyr^{1082}/Gln^{1112}$ and the degree of fibrosis progression (data not shown).

***Correlation Between NS5A Protein Sequence Polymorphism and HCC Development.*** NS5A protein sequences were obtained from 92% (45/49) and 74% (74/100) of pre-HCC and control isolates, respectively. Twenty-four (53%) of 45 pre-HCC isolates had IRRDR of 6 or more mutations (IRRDR≥6)

**Table 2. Correlation Between HCC and Sequence Polymorphic Factors of Core, NS3 and NS5A**

| HCV Protein | Factor | No. of Subjects / No. of Total* | | P Value |
|---|---|---|---|---|
| | | HCC | Control | |
| Core | Wild-core ($Arg^{70}$/ $Leu^{91}$) | 22/49 (45%) | 59/94 (63%) | 0.05 |
| | Non-wild-core | 27/49 (55%) | 35/94 (37%) | |
| | $Gln^{70}$ | 21/49 (43%) | 13/94 (14%) | 0.0002 |
| | Non-$Gln^{70}$ | 28/49 (57%) | 81/94 (86%) | |
| | $Leu^{91}$ | 37/49 (76%) | 70/94 (74%) | 1.0 |
| | Non- $Leu^{91}$ | 12/49 (24%) | 24/94 (26%) | |
| NS3 | $Tyr^{1082}$ / $Gln^{1112}$ | 29/46 (63%) | 39/93 (42%) | 0.029 |
| | Non-($Tyr^{1082}$ / $Gln^{1112}$) | 17/46 (37%) | 54/93 (58%) | |
| NS5A | IRRDR≥6 | 24/45 (53%) | 15/74 (20%) | 0.0003 |
| | IRRDR≤5 | 21/45 (47%) | 59/74 (80%) | |
| | ISDR≥3 | 11/45 (24%) | 8/74 (11%) | 0.07 |
| | ISDR≤2 | 34/45 (76%) | 66/74 (89%) | |
| | $Asn^{2218}$ | 11/45 (24%) | 3/74 (4%) | 0.002 |
| | Non-$Asn^{2218}$ | 34/45 (76%) | 71/74 (96%) | |

*Number of subjects with a given factor / total number of HCC or control. HCC, hepatocellular carcinoma; $Arg^{70}$, arginine at position 70 of the core protein; $Leu^{91}$, leucine at position 91 of the core protein; $Gln^{70}$, glutamine at position 70 of the core protein; $Tyr^{1082}$, tyrosine at position 1082 of NS3; $Gln^{1112}$, glutamine at position 1112 of NS3; IRRDR, interferon/ribavirin resistance-determining region; ISDR, interferon sensitivity-determining region; $Asn^{2218}$, asparagine at position 2218 of NS5A-ISDR.

while only 15 (20%) of 74 control isolates did (Table 2; $P = 0.0003$). We also found that pre-HCC isolates tended to have a higher degree of sequence heterogeneity in ISDR than control isolates, although not statistically significant due probably to the small number of cases examined; 11 (24%) of 45 pre-HCC isolates and 8 (11%) of 74 of control isolates had ISDR with three or more mutations ($P = 0.07$). Moreover, Asn at position 2218 ($Asn^{2218}$) within the ISDR was found in 24% (11/45) of pre-HCC isolates and only in 4% (3/74) of the control isolates ($P = 0.002$), suggesting that $Asn^{2218}$ is significantly associated with development of HCC.

***Cumulative HCC Incidence on the Basis of Core-$Gln^{70}$, NS3-$Tyr^{1082}$/$Gln^{1112}$, NS5A-IRRDR≥6, and NS5A-$Asn^{2218}$.*** Follow-up study revealed that the cumulative HCC incidence in patients infected with HCV-1b isolates with core protein of $Gln^{70}$ and those of non-$Gln^{70}$, respectively, was 29% and 5% at the end of 5 years, 56% and 23% at the end of 10 years, and 63% and 26% at the end of 15 years (Fig. 1A), with the differences between the two groups being statistically significant ($P < 0.0001$; Log-rank test). Likewise, the cumulative HCC incidence in patients infected with HCV-1b isolates with NS3 of $Tyr^{1082}$/$Gln^{1112}$ and those of non-($Tyr^{1082}$/$Gln^{1112}$), respectively, was 15% and 7% at the end of 5 years, 37% and 24% at the end of 10 years, and 45% and 24% at the end of 15 years ($P = 0.02$) (Fig. 1B). Also, the cumulative HCC incidence in patients infected with HCV-1b isolates of IRRDR≥6 and those of IRRDR≤5, respectively, was 18% and 10% at the end of 5 years, 59% and 22% at the end of 10 years, and 63% and 27% at the end of 15 years ($P = 0.0002$) (Fig. 1C). Similarly, the cumulative HCC incidence in patients infected with HCV-1b isolates of $Asn^{2218}$ and those of non-$Asn^{2218}$, respectively, was 31% and 9% at the end of 5 years, 77% and 28% at the end of 10 years, and 77% and 33% at the end of 15 years ($P = 0.0003$) (Fig. 1D).

***Identification of Independent Factors Correlated With HCC Development by Univariate and Multivariate Logistic Regression Analyses.*** In order to identify significant independent factors associated with HCC development, all available data of baseline patients' parameters and core, NS3, and NS5A polymorphic factors were first analyzed by univariate logistic analysis. This analysis yielded eight factors that were significantly associated with HCC development: core-$Gln^{70}$, NS3-($Tyr^{1082}$/$Gln^{1112}$), NS5A-IRRDR≥6, NS5A-$Asn^{2218}$, increased levels of ALT (>165 IU/L), AST (>65 IU/L), and AFP (>20 ng/L), and fibrosis staging score (≥3). Subsequently, those eight factors were entered in multivariate logistic regression analysis. This analysis identified two viral factors, core-$Gln^{70}$ and NS3-($Tyr^{1082}$/$Gln^{1112}$), and a host factor, AFP levels (>20 ng/L), as independent factors associated with HCC development (Table 3).

The vast majority of pre-HCC isolates (85%; 39/46) had core-$Gln^{70}$ and/or NS3-$Tyr^{1082}$/$Gln^{1112}$ and only 15% (7/46) had non-($Gln^{70}$ plus NS3-$Tyr^{1082}$/$Gln^{1112}$). By contrast, about a half of control isolates (52%; 46/89) had non-($Gln^{70}$ plus NS3-$Tyr^{1082}$/$Gln^{1112}$) (Fig. 2A). The difference in the proportion between HCC and control groups was statistically significant ($P < 0.0001$). Furthermore, the cumulative HCC incidence after 15-year follow-up was highest (63%) among patients with core-$Gln^{70}$ plus NS3-($Tyr^{1082}$/$Gln^{1112}$), whereas it was lowest (11%) among patients with non-($Gln^{70}$ plus NS3-$Tyr^{1082}$/$Gln^{1112}$) (Fig. 2B), with the difference being statistically significant ($P < 0.0001$; Log-rank test).

***Evolution of the Sequences of the Core, NS3, and NS5A Proteins During the Follow-up Period From Chronic Hepatitis to HCC Development.*** Finally, we investigated sequence evolution of the core protein, NS3 and NS5A (IRRDR and ISDR) during the follow-up period from chronic hepatitis to HCC development by comparing the sequences between pre-HCC and

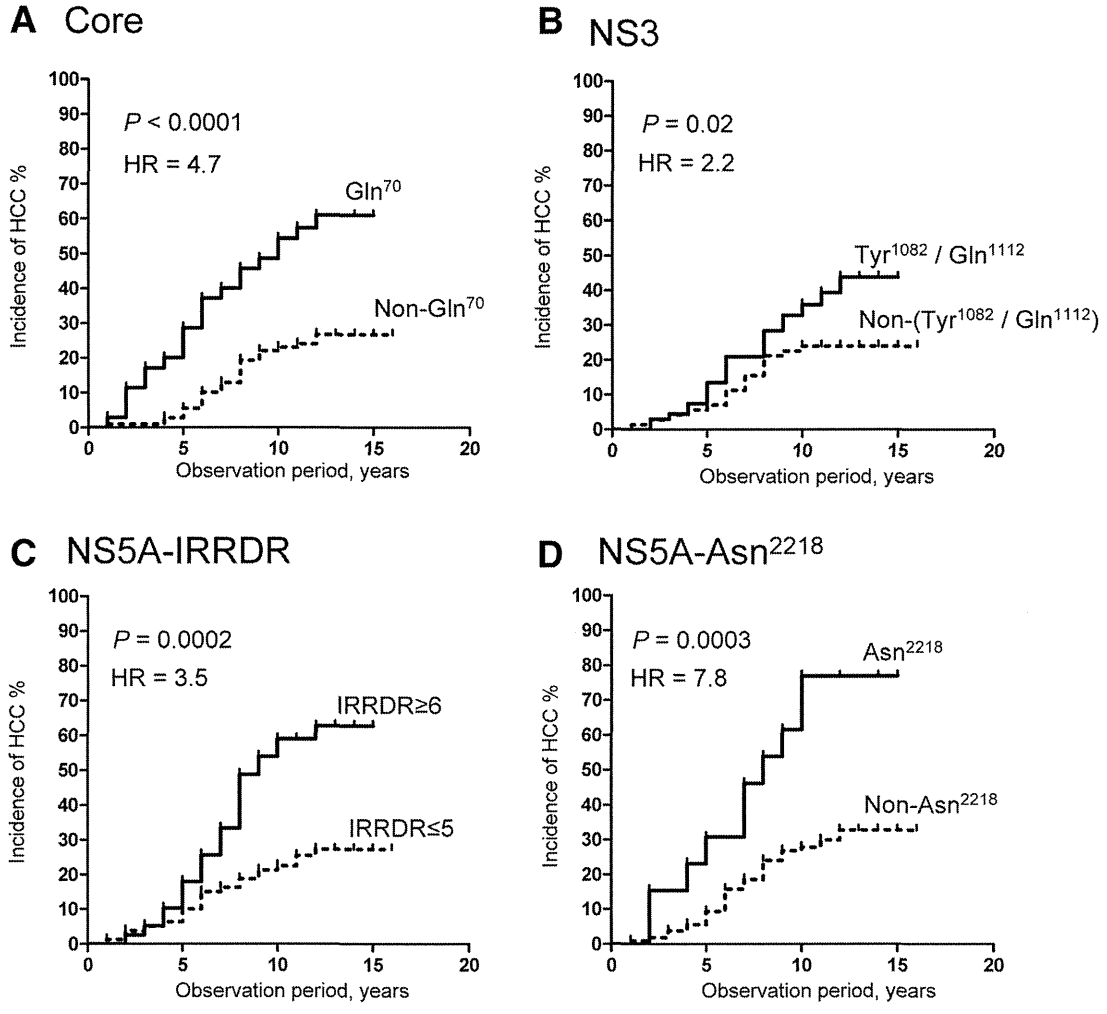


Fig. 1. Cumulative HCC incidence on the basis of HCV-1b sequence patterns. (A) Position 70 of the core protein. The numbers of core-$Gln^{70}$ and non-$Gln^{70}$ analyzed were 34 and 109, respectively. (B) Positions 1082 and 1112 of NS3. The numbers of NS3-($Tyr^{1082}$/$Gln^{1112}$) and non-($Tyr^{1082}$/$Gln^{1112}$) analyzed were 68 and 71, respectively. (C) NS5A-IRRDR. The numbers of NS5A-IRRDR≥6 and IRRDR≤5 analyzed were 39 and 80, respectively. (D) NS5A-$Asn^{2218}$. The numbers of NS5A-$Asn^{2218}$ and non-$Asn^{2218}$ analyzed were 14 and 105, respectively.

post-HCC isolates. The residue at position 70 of the core protein was conserved in 91% (41/45) of sequence pairs analyzed. The substitutions observed at this position were from $Arg^{70}$ and $His^{70}$ each to $Gln^{70}$ in two cases and from $Gln^{70}$ to $Arg^{70}$ in the other two cases. The residues at positions 1082 and 1112 of NS3 were conserved in 95% (41/43) and 100% (43/43), respectively, of the sequence pairs analyzed.

**Table 3. Univariate and Multivariate Regression Analyses to Identify Independent Factors Associated With HCC**

| | Univariate | | Multivariate | |
|---|---|---|---|---|
| **Variable** | **Odds Ratio (95% CI)** | ***P* Value** | **Odds Ratio (95% CI)** | ***P* Value** |
| Core-$Gln^{70}$ | 0.23 (0.10 - 0.52) | 0.0004 | 6.8 (2.1 - 23.0) | 0.001 |
| NS3-$Tyr^{1082}$ / $Gln^{1112}$ | 2.4 (1.1 - 4.9) | 0.029 | 3.4 (1.1 - 10.0) | 0.03 |
| NS5A-IRRDR≥6 | 4.5 (2.0 - 10.0) | 0.0003 | | |
| NS5A-$Asn^{2218}$ | 7.7 (2.0 - 29.0) | 0.002 | | |
| AFP (>20 ng/L) | 12 (5.1 - 30.0) | 0.0001 | 19.5 (4.7 - 80.0) | 0.0001 |
| ALT (>165 IU/L) | 4.0 (1.8 - 8.6) | 0.0006 | | |
| AST (>65 IU/L) | 3.9 (1.5 - 10.0) | 0.003 | | |
| Fibrosis staging score (≥3) | 2.4 (1.1 - 4.9) | 0.02 | | |

$Gln^{70}$, glutamine at position 70 of the core protein; $Tyr^{1082}$, tyrosine at position 1082 of NS3; $Gln^{1112}$, glutamine at position 1112 of NS3; IRRDR, interferon/ribavirin resistance-determining region; $Asn^{2218}$, asparagine at position 2218 of NS5A-ISDR, ALT, alanine aminotransferase; AST, aspartate transaminase; AFP; α-fetoprotein; IFN; interferon.

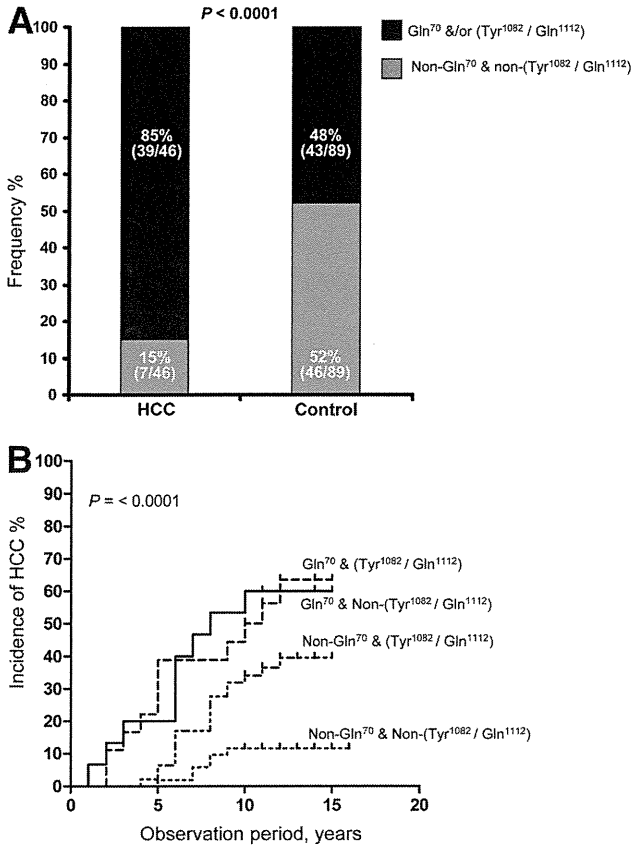


Fig. 2. (A) Proportions of HCV-1b isolates of the HCC high-risk group (core-Gln$^{70}$ and/or NS3-[Tyr$^{1082}$/Gln$^{1112}$]) and the low-risk group (non-Gln$^{70}$ and non-[Tyr$^{1082}$/Gln$^{1112}$]) among HCC and control groups. (B) Cumulative HCC incidence on the basis of different combined sequence patterns of position 70 of the core protein and positions 1082 and 1112 of NS3. Core-Gln$^{70}$ and NS3-(Tyr$^{1082}$/Gln$^{1112}$), n = 18; core-Gln$^{70}$ and non-(Tyr$^{1082}$/Gln$^{1112}$), n = 16; non-Gln$^{70}$ and NS3-(Tyr$^{1082}$/Gln$^{1112}$), n = 48; non-Gln$^{70}$/non-(Tyr$^{1082}$/Gln$^{1112}$), n = 53.

IRRDR and ISDR showed a high degree of sequence evolution. IRRDR sequences were different between pre-HCC and post-HCC isolates in 66% (25/38) of cases analyzed (Fig. 3). IRRDR sequences tended to be more polymorphic at the time of HCC occurrence. Frequency of HCV isolates with IRRDR≥6 was significantly higher in post-HCC isolates than in pre-HCC isolates; IRRDR≥6 was found in 47% (18/38) of post-HCC isolates compared to 24% (9/38) of pre-HCC isolates ($P = 0.03$). On the other hand, ISDR≥3 was found in 21% (8/38) of post-HCC isolates compared to 11% (4/38) of pre-HCC isolates, with the difference between the two groups being not statistically significant ($P = 0.3$).

## Discussion

HCC is one of the common long-term complications of HCV infection. However, whether HCV itself plays a direct role in the development of HCC and whether all HCV isolates are equally associated with HCC development remain to be determined. HCV core, NS3, and NS5A proteins have been reported to affect a wide variety of potentially oncogenic pathways in cell culture and experimental animal systems.[7] In the present study, we demonstrated that HCV isolates with core-Gln$^{70}$, NS3-Tyr$^{1082}$/Gln$^{1112}$ or NS5A-IRRDR≥6 were closely associated with HCC development. In addition, a follow-up study revealed that sequence patterns at position 70 of the core protein and positions 1082 and 1112 of NS3 did not significantly alter during the progression from chronic hepatitis to HCC while NS5A-IRRDR showed a significantly higher degree of sequence heterogeneity in post-HCC than in pre-HCC isolates.

Correlation between polymorphisms at positions 70 and 91 of HCV-1b core protein and IFN-based treatment outcome was extensively studied, especially in a Japanese population.[17-20] Interestingly, the same mutations were also associated with progression to HCC in the Japanese population with HCV-1b infection.[13] Results obtained in the present study confirmed and emphasized the significant association between the mutation at position 70 (core-Gln$^{70}$), but not at position 91, and HCC development (Tables 2, 3; Fig. 1A). Despite the clinical evidence that strongly supports the correlation between core-Gln$^{70}$ and HCC development, the molecular mechanism underlying this correlation is still obscure. Delhem et al.[36] found that tumor-derived HCV core proteins, but not nontumor-derived ones, interact with and activate double-stranded RNA-dependent protein kinase (protein kinase R or PKR), which might modulate viral persistence and carcinogenesis. Gln$^{70}$ was found in two of the three tumor-derived sequences, whereas Arg$^{70}$ was found in two of the three nontumor-derived ones.

As for the NS3 protein of HCV, the possible link between an N-terminal portion of NS3 encoding viral serine protease (aa 1027 to 1146) and hepatocarcinogenesis was reported.[21,22] However, information about the relationship between NS3 sequence diversity and HCC development is still limited. We previously reported a significant correlation between predicted secondary structure of an N-terminal portion of NS3 and HCC development.[34] In the present study, we demonstrated that HCV patients infected with HCV isolates with NS3-(Tyr$^{1082}$/Gln$^{1112}$) were at a higher risk to develop HCC than those infected with HCV isolates with non-Tyr$^{1082}$/Gln$^{1112}$ (Tables 2, 3; Fig. 2B). Computer-assisted secondary structure analysis of NS3 revealed that Tyr$^{1082}$ was associated with the

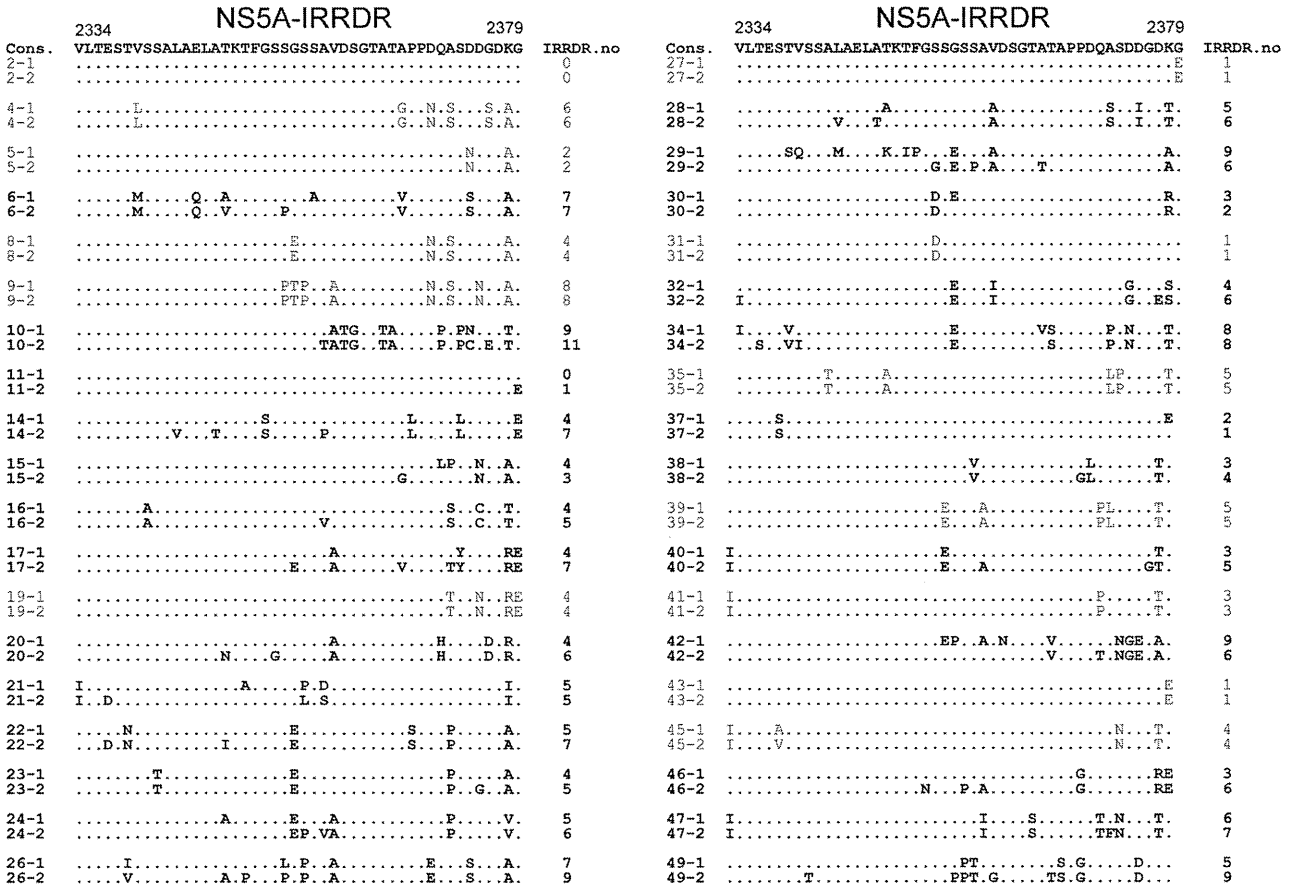


Fig. 3. Pairwise comparison of IRRDR sequences of HCV-1b during the follow-up period between chronic hepatitis and HCC development. Sequence pairs that differ between pre-HCC (numbered with -1) and post-HCC isolates (numbered with -2) are shown. The consensus sequence (Cons.) is shown at the top. The numbers along the sequence indicate the aa positions. Dots indicate residues identical to those of the Cons. sequence. The numbers of IRRDR mutations are shown on the right.

presence of a turn structure at around position 1083 while Phe[1082] was associated with the absence of the turn structure.[34] Notably, the catalytic triad of NS3 serine protease consists of His[1083], Asp[1107], and Ser[1165].[37] Since positions 1082 and 1112 are in close vicinity of the catalytic triad, sequences diversity at these positions might influence the serine protease activity and also pathogenicity of HCV. Large-scale, multicenter clinical studies as well as more detailed experimental studies at the molecular and cellular levels are needed to clarify the importance of sequence diversity at positions 1082 and 1112 of NS3 in HCV-mediated hepatocarcinogenesis.

HCV heterogeneity in NS5A-ISDR and NS5A-IRRDR are correlated with IFN-responsiveness.[17,18,25,26] As IFN-based therapy reduces the risk of HCC development,[4,28-30] we were interested to investigate whether there is a correlation between sequence heterogeneity in NS5A and development of HCC. Our present results revealed that a high degree of sequence heterogeneity in IRRDR (IRRDR≥6) was closely associated with HCC development (Table 2). We previously reported that IRRDR≥6 was significantly associated with good responses to PEG-IFN/RBV combination therapy.[26,27] These results collectively suggest that oncogenic properties and PEG-IFN/RBV responsiveness are independent viral characteristics and that PEG-IFN/RBV therapy helps eliminate oncogenic HCV isolates, thus reducing the risk of HCC development.

Position 2218 of NS5A, located within ISDR, appears to tolerate a wide range of aa substitutions as observed in different HCV-1b isolates.[25,38,39] Interestingly, Asn at position 2218 (Asn[2218]) was detected significantly more frequently in pre-HCC isolates than in the control isolates. Further studies are needed to determine the possible importance of this residue in hepatocarcinogenesis.

Another focus of attention is how the sequences of the core protein, NS3, and NS5A-IRRDR evolve during the interval between chronic hepatitis and HCC development. One of the significant advantages of the

present study was that we could conduct a longitudinal investigation by analyzing the target sequences of pre- and post-HCC isolates. We found that core-$Gln^{70}$ and NS3-($Tyr^{1082}$/$Gln^{1112}$) were well conserved in each paired sample. This indicates that core-$Gln^{70}$ and NS3-($Tyr^{1082}$/$Gln^{1112}$) were already present before the development of HCC. Non-$Gln^{70}$ of the core protein and non-$Tyr^{1082}$ and non-$Gln^{1112}$ of NS3 were also well conserved in each paired sample. These results imply the possibility that these sequence patterns were not a result of HCC but, rather, they were a possible causative factor for the development of HCC. We hypothesize, therefore, that HCV isolates with core-$Gln^{70}$ and/or NS3-($Tyr^{1082}$/$Gln^{1112}$) are highly oncogenic, whereas those with non-($Gln^{70}$ plus NS3-$Tyr^{1082}$/$Gln^{1112}$) are less oncogenic. It is not clear yet as to whether these oncogenic mutations were present from the very beginning of HCV infection or if they emerged at a certain timepoint (before the initiation of follow-up) during the long-term persistence through an adaptive viral evolution in the host. More comprehensive follow-up study is needed to address this issue. In any case, the core-$Gln^{70}$ and NS3-($Tyr^{1082}$/$Gln^{1112}$) would be considered an index for prediction of HCC development. On the other hand, IRRDR in NS5A is more tolerant for sequence evolution. IRRDR in post-HCC isolates showed a significantly higher degree of sequence heterogeneity compared with that in pre-HCC isolates. This observation suggests that IRRDR is under strong selective pressure during the course of HCV infection and that the high degree of IRRDR heterogeneity (IRRDR$\geq$6) in HCV isolates from patients with HCC may not be a causative factor for development of HCC.

In conclusion, the present results suggest the possibility that patients infected with HCV isolates with core-$Gln^{70}$ and/or NS3-($Tyr^{1082}$/$Gln^{1112}$) are at a higher risk to develop HCC compared to those with non-($Gln^{70}$ plus NS3-$Tyr^{1082}$/$Gln^{1112}$).

## References


1. Lauer GM, Walker BD. Hepatitis C virus infection. N Engl J Med 2001;345:41-52.
2. Niederau C, Lange S, Heintges T, Erhardt A, Buschkamp M, Hurter D, et al. Prognosis of chronic hepatitis C: results of a large, prospective cohort study. HEPATOLOGY 1998;28:1687-1695.
3. Ikeda K, Saitoh S, Suzuki Y, Kobayashi M, Tsubota A, Koida I, et al. Disease progression and hepatocellular carcinogenesis in patients with chronic viral hepatitis: a prospective observation of 2215 patients. J Hepatol 1998;28:930-938.
4. Yoshida H, Shiratori Y, Moriyama M, Arakawa Y, Ide T, Sata M, et al. Interferon therapy reduces the risk for hepatocellular carcinoma: national surveillance program of cirrhotic and noncirrhotic patients with chronic hepatitis C in Japan. IHIT Study Group. Inhibition of hepatocarcinogenesis by interferon therapy. Ann Intern Med 1999;131: 174-181.
5. Lok AS, Seeff LB, Morgan TR, di Bisceglie AM, Sterling RK, Curto TM, et al. Incidence of hepatocellular carcinoma and associated risk factors in hepatitis C-related advanced liver disease. Gastroenterology 2009;136:138-148.
6. Miki D, Ochi H, Hayes CN, Abe H, Yoshima T, Aikata H, et al. Variation in the DEPDC5 locus is associated with progression to hepatocellular carcinoma in chronic hepatitis C virus carriers. Nat Genet 2011; 43:797-800.
7. Banerjee A, Ray RB, Ray R. Oncogenic potential of hepatitis C virus proteins. Viruses 2010;2:2108-2133.
8. Marusawa H, Hijikata M, Chiba T, Shimotohno K. Hepatitis C virus core protein inhibits Fas- and tumor necrosis factor alpha-mediated apoptosis via NF-κB activation. J Virol 1999;73:4713-4720.
9. Ray RB, Meyer K, Ray R. Suppression of apoptotic cell death by hepatitis C virus core protein. Virology 1996;226:176-182.
10. Chang J, Yang SH, Cho YG, Hwang SB, Hahn YS, Sung YC. Hepatitis C virus core from two different genotypes has an oncogenic potential but is not sufficient for transforming primary rat embryo fibroblasts in cooperation with the H-*ras* oncogene. J Virol 1998;72: 3060-3065.
11. Ray RB, Lagging LM, Meyer K, Ray R. Hepatitis C virus core protein cooperates with ras and transforms primary rat embryo fibroblasts to tumorigenic phenotype. J Virol 1996;70:4438-4443.
12. Moriya K, Fujie H, Shintani Y, Yotsuyanagi H, Tsutsumi T, Ishibashi K, et al. The core protein of hepatitis C virus induces hepatocellular carcinoma in transgenic mice. Nat Med 1998;4:1065-1067.
13. Akuta N, Suzuki F, Kawamura Y, Yatsuji H, Sezaki H, Suzuki Y, et al. Amino acid substitutions in the hepatitis C virus core region are the important predictor of hepatocarcinogenesis. HEPATOLOGY 2007;46: 1357-1364.
14. Akuta N, Suzuki F, Hirakawa M, Kawamura Y, Sezaki H, Suzuki Y, et al. Amino acid substitutions in hepatitis C virus core region predict hepatocarcinogenesis following eradication of HCV RNA by antiviral therapy. J Med Virol 2011;83:1016-1022.
15. Akuta N, Suzuki F, Kawamura Y, Yatsuji H, Sezaki H, Suzuki Y, et al. Substitution of amino acid 70 in the hepatitis C virus core region of genotype 1b is an important predictor of elevated alpha-fetoprotein in patients without hepatocellular carcinoma. J Med Virol 2008;80: 1354-1362.
16. Kobayashi M, Akuta N, Suzuki F, Hosaka T, Sezaki H, Kobayashi M, et al. Influence of amino-acid polymorphism in the core protein on progression of liver disease in patients infected with hepatitis C virus genotype 1b. J Med Virol 2010;82:41-48.
17. El-Shamy A, Shoji I, Saito T, Watanabe H, Ide YH, Deng L, et al. Sequence heterogeneity of NS5A and core proteins of hepatitis C virus and virological responses to pegylated-interferon/ribavirin combination therapy. Microbiol Immunol 2011;55:418-426.
18. El-Shamy A, Kim SR, Ide YH, Sasase N, Imoto S, Deng L, et al. Polymorphisms of hepatitis C virus non-structural protein 5A and core protein and clinical outcome of pegylated-interferon/ribavirin combination therapy. Intervirology 2012;55:1-11.
19. Akuta N, Suzuki F, Sezaki H, Suzuki Y, Hosaka T, Someya T, et al. Association of amino acid substitution pattern in core protein of hepatitis C virus genotype 1b high viral load and non-virological response to interferon-ribavirin combination therapy. Intervirology 2005;48: 372-380.
20. Akuta N, Suzuki F, Kawamura Y, Yatsuji H, Sezaki H, Suzuki Y, et al. Predictive factors of early and sustained responses to peginterferon plus ribavirin combination therapy in Japanese patients infected with hepatitis C virus genotype 1b: amino acid substitutions in the core region and low-density lipoprotein cholesterol levels. J Hepatol 2007;46: 403-410.

21. Sakamuro D, Furukawa T, Takegami T. Hepatitis C virus nonstructural protein NS3 transforms NIH 3T3 cells. J Virol 1995;69:3893-3896.
22. Zemel R, Gerechet S, Greif H, Bachmatove L, Birk Y, Golan-Goldhirsh A, et al. Cell transformation induced by hepatitis C virus NS3 serine protease. J Viral Hepat 2001;8:96-102.
23. Fujita T, Ishido S, Muramatsu S, Itoh M, Hotta H. Suppression of actinomycin D-induced apoptosis by the NS3 protein of hepatitis C virus. Biochem Biophys Res Commun 1996;229:825-831.
24. Macdonald A, Harris M. Hepatitis C virus NS5A: tales of a promiscuous protein. J Gen Virol 2004;85:2485-2502.
25. Enomoto N, Sakuma I, Asahina Y, Kurosaki M, Murakami T, Yamamoto C, et al. Mutations in the nonstructural protein 5A gene and response to interferon in patients with chronic hepatitis C virus 1b infection. N Engl J Med 1996;334:77-81.
26. El-Shamy A, Nagano-Fujii M, Sasase N, Imoto S, Kim SR, Hotta H. Sequence variation in hepatitis C virus nonstructural protein 5A predicts clinical outcome of pegylated interferon/ribavirin combination therapy. HEPATOLOGY 2008;48:38-47.
27. Kim SR, El-Shamy A, Imoto S, Kim KI, Ide YH, Deng L, et al. Prediction of response to pegylated interferon/ribavirin combination therapy for chronic hepatitis C genotype 1b and high viral load. J Gastroenterol 2012;47:1143-1151.
28. Ikeda K, Saitoh S, Arase Y, Chayama K, Suzuki Y, Kobayashi M, et al. Effect of interferon therapy on hepatocellular carcinogenesis in patients with chronic hepatitis type C: A long-term observation study of 1,643 patients using statistical bias correction with proportional hazard analysis. HEPATOLOGY 1999;29:1124-1130.
29. Okanoue T, Itoh Y, Minami M, Sakamoto S, Yasui K, Sakamoto M, et al. Interferon therapy lowers the rate of progression to hepatocellular carcinoma in chronic hepatitis C but not significantly in an advanced stage: a retrospective study in 1148 patients. Viral Hepatitis Therapy Study Group. J Hepatol 1999;30:653-659.
30. Benvegnu L, Chemello L, Noventa F, Fattovich G, Pontisso P, Alberti A. Retrospective analysis of the effect of interferon therapy on the clinical outcome of patients with viral cirrhosis. Cancer 1998;83:901-909.
31. Okamoto H, Sugiyama Y, Okada S, Kurai K, Akahane Y, Sugai Y, et al. Typing hepatitis C virus by polymerase chain reaction with type-specific primers: application to clinical surveys and tracing infectious sources. J Gen Virol 1992;73:673-679.
32. El-Shamy A, Sasayama M, Nagano-Fujii M, Sasase N, Imoto S, Kim SR, et al. Prediction of efficient virological response to pegylated interferon/ribavirin combination therapy by NS5A sequences of hepatitis C virus and anti-NS5A antibodies in pre-treatment sera. Microbiol Immunol 2007;51:471-482.
33. Ogata S, Nagano-Fujii M, Ku Y, Yoon S, Hotta H. Comparative sequence analysis of the core protein and its frameshift product, the F protein, of hepatitis C virus subtype 1b strains obtained from patients with and without hepatocellular carcinoma. J Clin Microbiol 2002;40:3625-3630.
34. Ogata S, Florese RH, Nagano-Fujii M, Hidajat R, Deng L, Ku Y, et al. Identification of hepatitis C virus (HCV) subtype 1b strains that are highly, or only weakly, associated with hepatocellular carcinoma on the basis of the secondary structure of an amino-terminal portion of the HCV NS3 protein. J Clin Microbiol 2003;41:2835-2841.
35. Kato N, Hijikata M, Ootsuyama Y, Nakagawa M, Ohkoshi S, Sugimura T, et al. Molecular cloning of the human hepatitis C virus genome from Japanese patients with non-A, non-B hepatitis. Proc Natl Acad Sci U S A 1990;87:9524-9528.
36. Delhem N, Sabile A, Gajardo R, Podevin P, Abadie A, Blaton MA, et al. Activation of the interferon-inducible protein kinase PKR by hepatocellular carcinoma derived-hepatitis C virus core protein. Oncogene 2001;20:5836-5845.
37. Love RA, Parge HE, Wickersham JA, Hostomsky Z, Habuka N, Moomaw EW, et al. The crystal structure of hepatitis C virus NS3 proteinase reveals a trypsin-like fold and a structural zinc binding site. Cell 1996;87:331-342.
38. Saiz JC, Lopez-Labrador FX, Ampurdanes S, Dopazo J, Forns X, Sanchez-Tapias JM, et al. The prognostic relevance of the nonstructural 5A gene interferon sensitivity determining region is different in infections with genotype 1b and 3a isolates of hepatitis C virus. J Infect Dis 1998;177:839-847.
39. Sarrazin C, Berg T, Lee JH, Teuber G, Dietrich CF, Roth WK, et al. Improved correlation between multiple mutations within the NS5A region and virological response in European patients chronically infected with hepatitis C virus type 1b undergoing combination therapy. J Hepatol 1999;30:1004-1013.

Biochemical and Biophysical Research Communications 434 (2013) 803–808

Contents lists available at SciVerse ScienceDirect

Biochemical and Biophysical Research Communications

journal homepage: www.elsevier.com/locate/ybbrc

# Distinct DDX DEAD-box RNA helicases cooperate to modulate the HIV-1 Rev function

Mariko Yasuda-Inoue, Misao Kuroki, Yasuo Ariumi *

*Center for AIDS Research, Kumamoto University, Kumamoto 860-0811, Japan*

ARTICLE INFO

*Article history:*
Received 19 March 2013
Available online 19 April 2013

*Keywords:*
HIV-1
Rev
DDX3
DDX5
RNA helicase
RNA export

ABSTRACT

RNA helicase plays an important role in host mRNA and viral mRNA transcription, transport, and translation. Many viruses utilize RNA helicases in their life cycle, while human immunodeficiency virus type 1 (HIV-1) does not encode an RNA helicase. Thus, host RNA helicase has been involved in HIV-1 replication. Indeed, DDX1 and DDX3 DEAD-box RNA helicases are known to be required for efficient HIV-1 Rev-dependent RNA export. However, it remains unclear whether distinct DDX RNA helicases cross-talk and cooperate to modulate the HIV-1 Rev function. In this study, we noticed that distinct DDX RNA helicases, including DDX1, DDX3, DDX5, DDX17, DDX21, DDX56, except DDX6, bound to the Rev protein and they colocalized with Rev in nucleolus or nucleus. In this context, these DEAD-box RNA helicases except DDX6 markedly enhanced the HIV-1 Rev-dependent RNA export. Furthermore, DDX3 interacted with DDX5 and synergistically enhanced the Rev function. As well, combination of other distinct DDX RNA helicases cooperated to stimulate the Rev function. Altogether, these results suggest that distinct DDX DEAD-box RNA helicases cooperate to modulate the HIV-1 Rev function.



## 1. Introduction

Human immunodeficiency virus type 1 (HIV-1) is a retrovirus of the lentivirus genus with a positive strand RNA genome of 9 kb which encodes nine polypeptides, three structural proteins, Gag (group-specific antigen), Pol (polymerase) and Env (envelope), the accessory proteins, Vif, Vpu, Vpr, and Nef, and the regulatory proteins, Tat and Rev. The gene expression of HIV-1 is regulated transcriptionally by Tat through its binding to a nascent viral *trans*-activation responsive (TAR) RNA [1,2], and post-transcriptionally by Rev through its association with Rev-responsive element (RRE) RNA in the *env* gene [3–5]. Both Tat and Rev interact with several host factors in their transcriptional and post-transcriptional functions [1–6].

Since the intron-containing host RNA cannot leave the nucleus before it is completely spliced, HIV-1 needs to evade this form of host surveillance to export unspliced or partially spliced viral RNA into cytoplasm and produce HIV-1 structural proteins and accessory proteins. For this, Rev contains a classical leucine-rich nuclear export signal (NES) that recruits nuclear export receptor CRM1 [3–5]. Upon binding to the RRE together with the GTP-bound form of Ran, CRM1 forms the export complex and Rev/CRM1/RanGTP complex exports unspliced or partially spliced viral RNA from the nucleus to the cytoplasm [3–5].

Helicases are enzymes that hydrolyze nucleotide triphosphates (NTPs) and use the energy to unwind nucleic acid duplexes or to translocate along the nucleic acid strand. Depending on whether helicases unwind RNA or DNA duplexes, helicases are classified into RNA helicases and DNA helicases. Exceptionally, RNA helicase A (RHA) can unwind both RNA and DNA. DEAD (D-E-A-D: Asp-Glu-Ala-Asp)-box RNA helicases, which are ATPase-dependent RNA helicases and are found in all organisms from bacteria to humans, are involved in various RNA metabolic processes, including transcription, translation, RNA splicing, RNA transport, and RNA degradation [7,8]. Many viruses utilize RNA helicases in their life cycle. Indeed, we recently found that DDX3 and DDX6, DEAD-box RNA helicases, are required for hepatitis C virus (HCV) RNA replication [9,10]. In addition to DDX3 and DDX6, DDX5 binds to HCV NS5B RNA-dependent RNA polymerase and it is involved in the HCV replication [11,12]. Furthermore, DDX21 plays an important role in the translational control of a Borna disease virus (BDV) polycistronic mRNA [13]. Moreover, the capsid-binding nucleolar helicase DDX56 is important for infectivity of West Nile virus [14]. On the other hand, several viruses carry their own RNA helicases to assist the synthesis of their genome, such as HCV, flavivirus, severe acute respiratory syndrome (SARS) coronavirus, rubella virus, and alphavirus, however, HIV-1 does not encode an RNA helicase [15,16]. Thus, host RNA helicases may be involved in HIV-1 replication [15,17]. In fact, DDX1 and DDX3 have been implicated in the rep-

* Corresponding author. Address: Center for AIDS Research, Kumamoto University, 2-2-1, Honjo, Chuo-ku, Kumamoto 860-0811, Japan. Fax: +81 96 373 6834.
*E-mail address:* ariumi@kumamoto-u.ac.jp (Y. Ariumi).

0006-291X/$ - see front matter Crown Copyright © 2013 Published by Elsevier Inc. All rights reserved.
http://dx.doi.org/10.1016/j.bbrc.2013.04.016

lication of HIV-1 replication [18–22]. Both DDX1 and DDX3 interact with HIV-1 Rev and enhance Rev-dependent HIV-1 nuclear export [18–22]. However, the role of cross talk of these DDX or other DDX DEAD-box RNA helicases is still unknown. To address this issue, we first examined whether distinct DDX RNA helicases cooperate to modulate the HIV-1 Rev function and these DDX interact with Rev.

## 2. Material and methods

### 2.1. Cell culture

293FT cells were cultured in Dulbecco's modified Eagle's medium (DMEM; Invitrogen, Carlsbad, CA, USA) supplemented with 10% fetal bovine serum (FBS).

### 2.2. Plasmid construction

To construct pcDNA3-HA-DDX1, pcDNA3-HA-DDX5, pcDNA-HA-DDX6, pcDNA3-HA-DDX17, pcDNA3-HA-DDX21, pcDNA3-HA-DDX56, or pcDNA3-FLAG-DDX5, a DNA fragment encoding DDX1, DDX5, DDX6, DDX17, DDX21, or DDX56 was amplified from total RNAs by reverse transcription (RT)-PCR using KOD-Plus DNA polymerase (TOYOBO, Osaka, Japan) and the following pairs of primers: DDX1, 5′-CGGGATCCAAGATGGCGGCCTTCTCCGAGAT GGGTGTAATG (Forward), 5′-CCGCTCGAGTCAGAAGGTTCTGAA-CAGCTGGTTAGGAAG-3′ (Reverse); DDX5, 5′-CGGGATCCAAGAT-GTCGGGTTATTCGAGTGACCGAGACCGC-3′ (Forward), 5′-CCGCT CGAGTTATTGGGAATATCCTGTTGGCATTGGATA-3′ (Reverse); DDX6, 5′-CGGGATCCAAGATGAGCACGGCCAGAACAGAGAACCC TGTT-3′ (Forward), 5′-CCGCTCGAGTTAAGGTTTCTCATCTTCTA-CAGGCTCGCT-3′ (Reverse); DDX17, 5′-CGGGATCCAAGATGCCC ACCGGCTTTGTAG-3′ (Forward), 5′-CCGGCGGCCGCTCATTTACGT-GAAGGAGGA-3′ (Reverse); DDX21, 5′-CGGGATCCAAGATGCCGG-GAAAACTCCGTAGTGACGCTGGT-3′ (Forward), 5′-CCGCTCGA GTTATTGACCAAATGCTTTACTGAAACTCCG-3′ (Reverse); DDX56, 5′-CGGGATCCAAGATGGAGGACTCTGAAGCACT-3′ (Forward), 5′-CCGGCGGCCGCTCAGGAGGGCTTGGCTGTGGGTC-3′ (Reverse).

The obtained DNA fragments were subcloned into either *Bam*HI-*Xho*I or *Bam*HI-*Not*I site of the pcDNA3-HA or pcDNA3-FLAG vector [23], and the nucleotide sequences were determined. We previously described pHA-DDX3 [9,18].

### 2.3. Luciferase assay

Plasmids were transfected into 293FT cells ($2 \times 10^4$ cells) using the FuGENE 6 transfection reagent (Promega, Madison, WI, USA). Luciferase assays were performed 24 h after transfection using luciferase assay reagent according to the manufacturer's instructions (Promega). All transfections utilized equal total amounts of plasmid DNA quantities owing to the addition of empty vector into the transfection mixture. Results were obtained through three independent transfections. A lumat LB9507 luminometer (Berthold, Bad Wildbad, Germany) was used to detect the luciferase activity.

### 2.4. Western blot analysis

Cells were lysed in buffer containing 50 mM Tris–HCl (pH 8.0), 150 mM NaCl, 4 mM EDTA, 1% Nonidet P (NP)-40, 0.1% sodium dodecyl sulfate (SDS), 1 mM dithiothreitol (DTT) and 1 mM phenylmethylsulfonyl fluoride (PMSF). Supernatants from these lysates were subjected to SDS–polyacrylamide gel electrophoresis, followed by immunoblot analysis using anti-HIV Rev (A2-832; Icosagen, Tartu, Estonia), anti-HA (HA-7; Sigma, Saint Louis, MI, USA), anti-DDX5 (A300-523A; Bethyl), or anti-FLAG antibody (M2, Sigma).

### 2.5. Immunoprecipitation

Cells were lysed in buffer containing 10 mM Tris–HCl (pH 8.0), 150 mM NaCl, 4 mM EDTA, 0.1% NP-40, 10 mM NaF, 1 mM DTT and 1 mM PMSF. Lysates were pre-cleared with 30 μl of protein-G-Sepharose (GE Healthcare Bio-Sciences, Uppsala, Sweden). Pre-cleared supernatants were incubated with 5 μg of anti-HA antibody (3F10; Roche Diagnostics, Mannheim, Germany) at 4 °C for 1 h. Following absorption of the precipitates on 30 μl of protein-G-Sepharose resin for 1 h, the resin was washed four times with 700 μl lysis buffer. Proteins were eluted by boiling the resin for 5 min in 2X Laemmli sample buffer. The proteins were then subjected to SDS–PAGE, followed by immunoblotting analysis using anti-HA, anti-FLAG, or anti-HIV-1 Rev antibody.

### 2.6. Immunofluorescence and confocal microscopic analysis

Cells were fixed in 3.6% formaldehyde in phosphate-buffered saline (PBS), permeabilized in 0.1% Nonidet P-40 in PBS at room temperature, and incubated with anti-DDX1 (IHC-00132; Bethyl, Montgomery, TX, USA), anti-DDX5 (A300-523A; Bethyl), anti-DDX6 (A300-460A; Bethyl), anti-DDX17 (A300-509A; Bethyl), anti-DDX21 (A300-627A; Bethyl), anti-DDX56 (A302-978A; Bethyl), anti-DDX3 (IN and NT; AnaSpec, San Jose, CA, USA), anti-DDX3X (LS-C64576; LifeSpan BioSciences, Seattle, WA, USA), and anti-HIV-1 Rev antibody (A2-832; Icosagen) at a 1:300 dilution in PBS containing 3% bovine serum albumin (BSA) at 37 °C for 30 min. They were then stained with Cy3-conjugated anti-mouse antibody and either fluorescein isothiocyanate (FITC)-conjugated anti-rabbit antibody (Jackson ImmunoResearch, West Grove, PA) or Alexa Fluor 647 anti-rabbit IgG (Molecular Probes, Invitrogen) at a 1:300 dilution in PBS containing BSA at 37 °C for 30 min. Nuclei were stained with DAPI (4′, 6′-diamidino-2-phenylindole). Following extensive washing in PBS, the cells were mounted on slides using a mounting media of SlowFade Gold antifade reagent (Invitrogen) added to reduce fading. Samples were viewed under a confocal laser-scanning microscope (FV1000; Olympus, Tokyo, Japan).

## 3. Results

### 3.1. Distinct DDX RNA helicaes interact with HIV-1 Rev and enhance the Rev function

To investigate the potential role of distinct DDX DEAD-box RNA helicases in HIV-1 Rev function, we first used the Rev-dependent luciferase-based reporter plasmid pDM628 [19,20,24] (Fig. 1A). As previously described, luciferase production was markedly stimulated by Rev, which induced a 15-fold increase in reporter signal (Fig. 1A). Then, 293FT cells were cotransfected with several HA-tagged DDX, including DDX1, DDX3, DDX5, DDX6, DDX17, DDX21, DDX56, pDM628, and/or Rev expression plasmid. While each DDX alone had no effect or marginal effect on the Rev-dependent luciferase-based reporter pDM628 in the absence of Rev (data not shown), all DDX synergized to stimulate the luciferase levels with Rev, respectively (Fig. 1B). Indeed, DDX1, DDX3, or DDX5 markedly enhanced the Rev function, while DDX6 had a marginal effect. Thus, distinct DDX RNA helicases seemed to regulate HIV-1 Rev function. Since both DDX1 and DDX3 interact with HIV-1 Rev and enhance Rev-dependent HIV-1 nuclear export [18–22], other DDX RNA helicases also might bind to Rev. To probe this possibility, we performed co-immunoprecipitation analyses on extracts of 293FT cells expressing Rev and HA-tagged DDX3, DDX5,

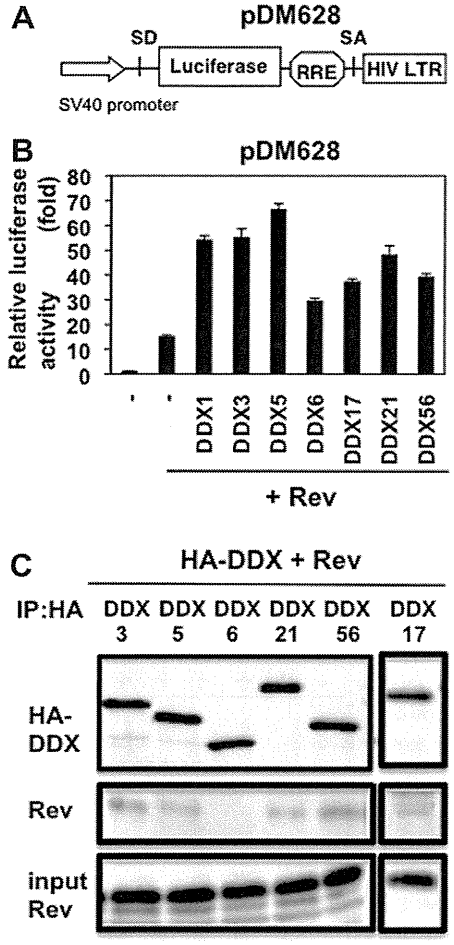


**Fig. 1.** Distinct DDX DEAD-box RNA helicases enhance HIV-1 Rev function. (A) Schematic representation of the Rev-dependent luciferase-based reporter plasmid pDM628 harboring a splice donor (SD), splice acceptor (SA), and Rev-responsive element (RRE). (B) 293FT cells ($2 \times 10^4$ cells) were cotransfected with pDM628 (100 ng), pcDNA3-HA-DDX1, pHA-DDX3, pcDNA3-HA-DDX5, pcDNA3-HA-DDX6, pcDNA3-HA-DDX17, pcDNA3-HA-DDX21, or pcDNA3-HA-DDX56 (100 ng), and/or pcRev (100 ng). 24 h after transfection, luciferase activity in the cellular lysates was measured. Results are from three independent experiments. (C) 293FT cells were cotransfected with pHA-DDX3 (4 μg), pcDNA3-HA-DDX5, pcDNA3-HA-DDX6, pcDNA3-HA-DDX17, pcDNA3-HA-DDX21, or pcDNA3-HA-DDX56, and pcRev (4 μg). The cell lysates were immunoprecipitated with an anti-HA antibody, followed by immunoblot analysis using either anti-HA or anti-Rev antibody.

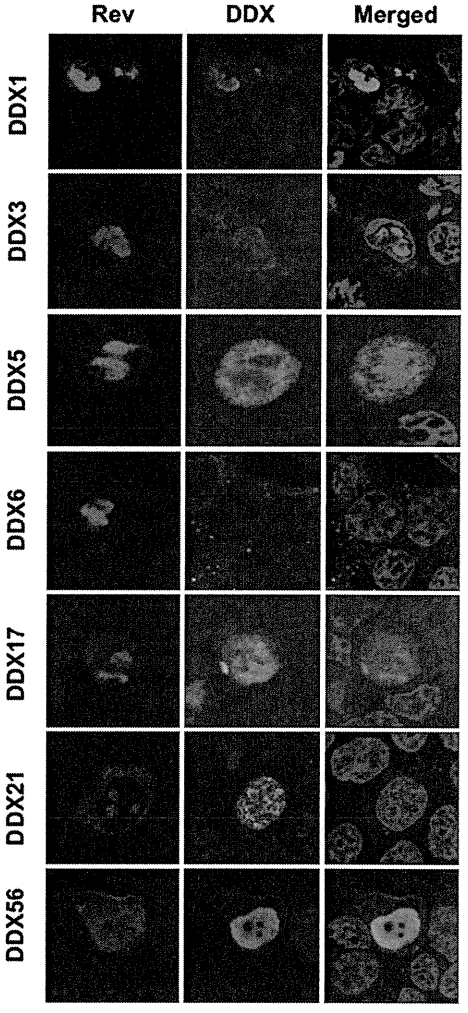


**Fig. 2.** Subcellular localization of DDX and Rev in 293FT cells. 293FT cells were cotransfected with pcDNA3-HA-tagged DDX1, DDX3, DDX5, DDX17, DDX21, or DDX56 (200 ng), and pcRev (200 ng). Cells were stained with anti-Rev and anti-DDX1, anti-DDX3, anti-DDX5, anti-DDX6, anti-DDX17, anti-DDX21, or anti-DDX56 antibodies 24 h after transfection and then visualized with Cy3 (Rev) or FITC (DDX). Nuclei were stained with DAPI. Images were visualized by using confocal laser scanning microscopy. The right panels exhibit the two-color overlay images (Merged).

DDX6, DDX17, DDX21, or DDX56 (Fig. 1C). Consequently, Rev and HA-DDX3, HA-DDX5, HA-DDX21, or HA-DDX56 could be immunoprecipitated with anti-HA antibody, indicating that Rev formed a complex with DDX3, DDX5, DDX17, DDX21, or DDX56, whether directly or indirectly. Importantly, Rev and DDX6 could not be immunoprecipitated, suggesting that Rev does not bind to DDX6 (Fig. 1C). Thus, we confirmed that several DDX DEAD-box RNA helicases except DDX6 could bind to Rev.

Then, we examined subcellular localization of Rev and HA-tagged DDX1, DDX3, DDX5, DDX6, DDX17, DDX21, or DDX56 in 293FT cells using confocal laser scanning microscopy (Fig. 2). Consequently, we observed that Rev predominantly localized in nucleolus. Both DDX1 and DDX3 colocalized with Rev in nucleolus and DDX3 also distributed in the cytoplasm. DDX5 mostly localized in nucleus and seemed to be partially colocalized with Rev in nucleus and nucleolus, while DDX6 predominantly localized in cytoplasmic speckles termed processing (P)-bodies. Consistent with the finding by immunoprecipitation analysis (Fig. 1C), DDX6 did not colocalize with Rev. Furthermore, DDX17 localized in both nucleus and nucleolus and DDX17 partially colocalized with Rev in the nucleolus. Moreover, DDX21 localized in nucleolus and DDX21 partially colocalized with Rev in the perinucleolar region. Notably, DDX56 altered the subcellular localization of Rev from nucleolus to nucleus and it mostly colocalized with Rev in the nucleus. Thus, several DDX RNA helicases except DDX6 could mostly or partially colocalize with Rev in the nucleolus or nucleus, suggesting that distinct DDX RNA helicases interact with Rev.

### 3.2. Distinct DDX RNA helicases cooperate to enhance the Rev function

To examine whether DDX3 and DDX5 cooperate to modulate the HIV-1 Rev function, 293FT cells were cotransfected with HA-tagged DDX3, HA-DDX5, pDM628, and/or Rev expression plasmid. When both DDX3 and DDX5 were co-expressed, they synergistically enhanced the Rev function (Fig. 3A), suggesting that DDX3 and DDX5 cooperate to enhance the Rev function. To probe the mechanism of this phenomenon, we performed co-immunoprecipitation analyses on extracts of 293FT cells expressing HA-tagged

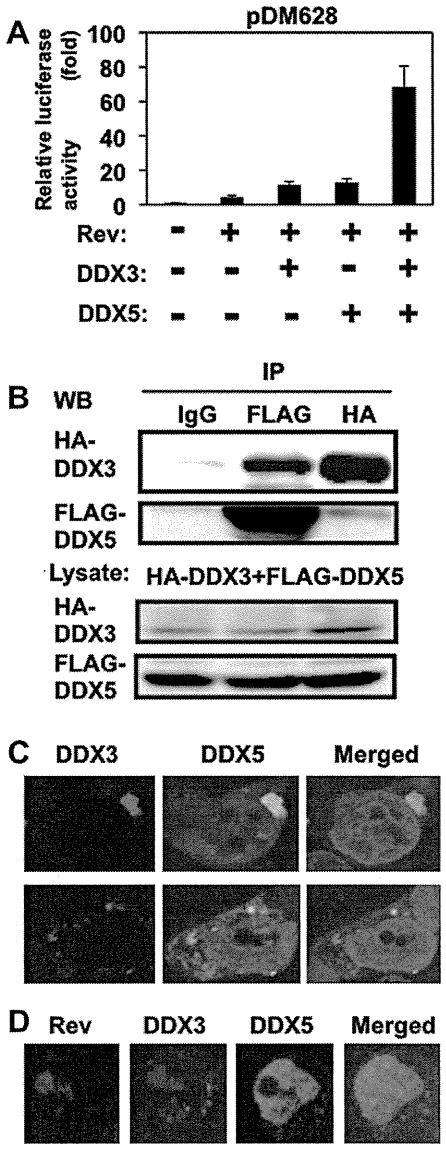


**Fig. 3.** DDX3 and DDX5 cooperates to enhance Rev function. (A) 293FT cells ($2 \times 10^4$ cells) were cotransfected with pDM628 (100 ng), pcRev (50 ng), pHA-DDX3 (100 ng), and/or pcDNA3-HA-DDX5 (100 ng). 24 h after transfection, luciferase activity in the cellular lysates was measured. Results are from three independent experiments. (B) 293FT cells were cotransfected with pHA-DDX3 (4 μg) and pcDNA3-FLAG-DDX5 (4 μg). The cell lysates were immunoprecipitated with an anti-HA, anti-FLAG antibody, or normal mouse IgG, followed by immunoblot analysis using either anti-HA or anti-FLAG antibody. (C) DDX3 colocalizes with DDX5. 293FT cells cotransfected with pHA-DDX3 (200 ng) and pcDNA3-FLAG-DDX5 (200 ng) were examined by confocal laser scanning microscopy. Cells were stained with anti-DDX3 (LS-C64576; LifeSpan) and anti-DDX5 antibodies and then visualized with Cy3 (DDX3) or FITC (DDX5). (D) 293FT cells cotransfected with pcRev (200 ng), pHA-DDX3 (200 ng), and pcDNA3-FLAG-DDX5 (200 ng) were stained with FITC-conjugated anti-HA, anti-Rev, or anti-DDX5 antibody and then visualized with Cy3 (Rev), FITC (DDX3) or Far-red/Alexa Fluor 647 (DDX5). (For interpretation of the references to colour in this figure legend, the reader is referred to the web version of this article.)

DDX3 and FLAG-tagged DDX5 (Fig. 3B). Consequently, HA-DDX3 and FLAG-DDX5 could be co-immunoprecipitated with anti-HA or anti-FLAG antibody, indicating that DDX3 formed a complex with DDX5 whether directly or indirectly. Furthermore, DDX3 mostly colocalized with DDX5 in cytoplasmic speckles in the perinuclear region (Fig. 3C). Moreover, DDX3 relocalized and colocalized with Rev in nucleolus and DDX3 also colocalized with DDX5

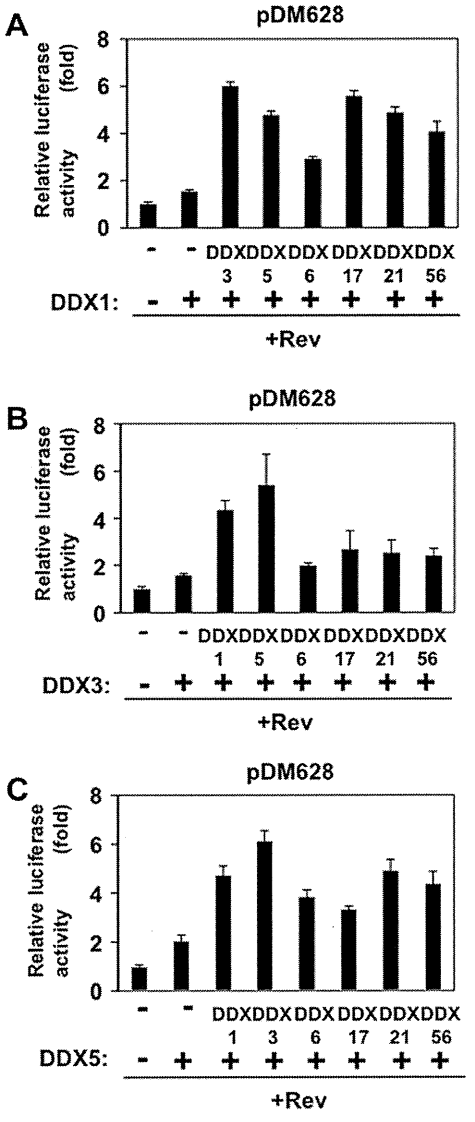


**Fig. 4.** Combination of distinct DDX RNA helicases cooperate to enhance the Rev function. (A–C) 293FT cells ($2 \times 10^4$ cells) were cotransfected with pDM628 (100 ng), pcRev (100 ng) and/or combination with pcDNA3-HA-DDX1, pHA-DDX3, pcDNA3-HA-DDX5, pcDNA3-HA-DDX6, pcDNA3-HA-DDX17, pcDNA3-HA-DDX21, and/or pcDNA3-HA-DDX56 (100 ng). 24 h after transfection, luciferase activity in the cellular lysates was measured. Results are from three independent experiments.

in the cytoplasmic speckles, when DDX3, DDX5, and Rev were co-expressed in 293FT cells (Fig. 3D). Although DDX5 mostly localized in the nucleus, it faintly localized in the nucleolus as well as in the cytoplasmic speckles (Fig. 3D). Thus, Rev could interact with both DDX3 and DDX5.

To further confirm the cooperation of distinct DDX DEAD-box RNA helicases in the Rev function, we examined the luciferase assays with various combination series of distinct DDX, including DDX1, DDX3, DDX5, DDX6, DDX17, DDX21, and DDX56 (Fig. 4). In this context, we found that several combination of DDX (DDX1 and DDX3; DDX1 and DDX5; DDX3 and DDX5; DDX5 and DDX21) could synergistically enhance the Rev function (Fig. 4A–C).

## 4. Discussion

So far, it has been indicated that host RNA helicases may be involved in HIV-1 replication at multiple stages, such as the reverse transcription of HIV-1 RNA, HIV-1 mRNA transcription, the nu-